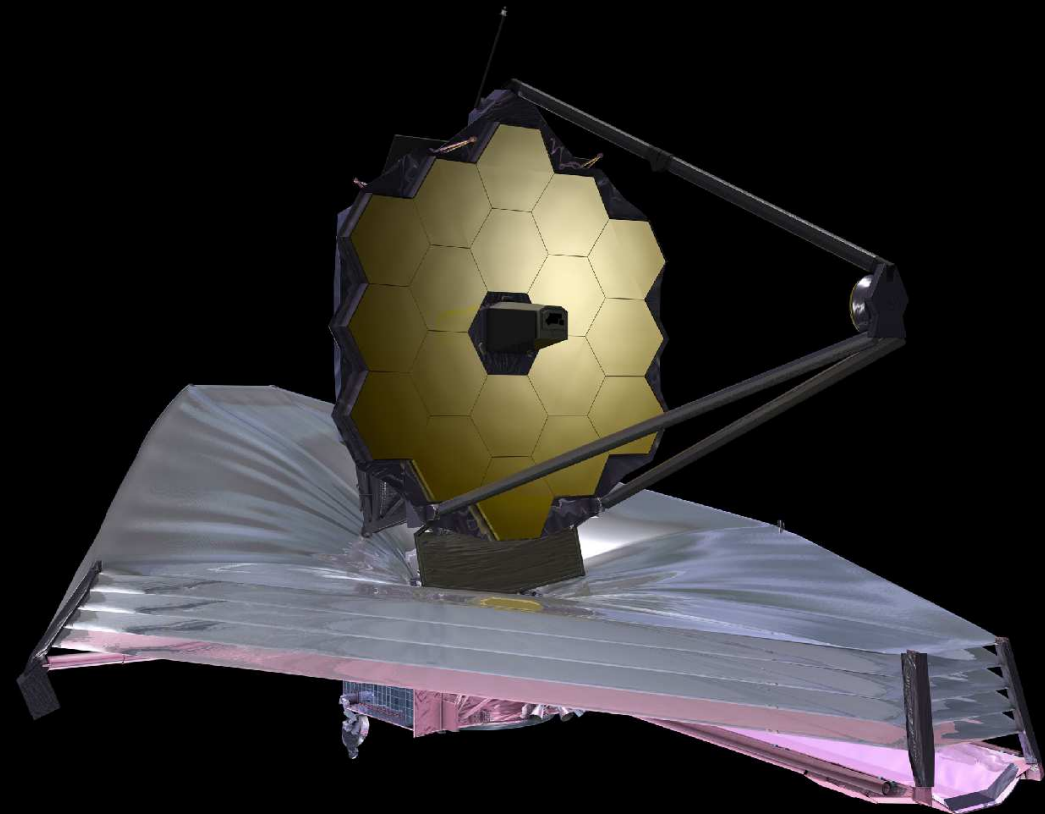


HST Observations of LyC Radiation from Galaxies & weak AGN at $2.3 \lesssim z \lesssim 5$: (How) Did they Reionize the Universe?

Rogier Windhorst (ASU) — JWST Interdisciplinary Scientist

Brent Smith, S. Cohen, R. Jansen, L. Jiang, M. Dijkstra, A. Inoue,

A. Koekemoer, R. Bielby, J. MacKenty, R. O'Connell, & J. Silk



Talk at Tel Aviv University, Monday May 25, 2015 (Tel Aviv, Israel)

All presented materials are ITAR-cleared.

Outline

- (1) HST Wide Field Camera 3 Data & Spectroscopic Sample Selection
- (2) WFC3 & ACS Lyman Continuum Stacking, Systematics, & Fluxes
- (3) Stacked UV and Lyman Continuum Light-Profiles
- (4) SED-fitting & Dust (A_V)-distribution
- (5) LyC Escape Fractions vs. z for Faint Galaxies & Weak AGN
- (6) Summary and Conclusions



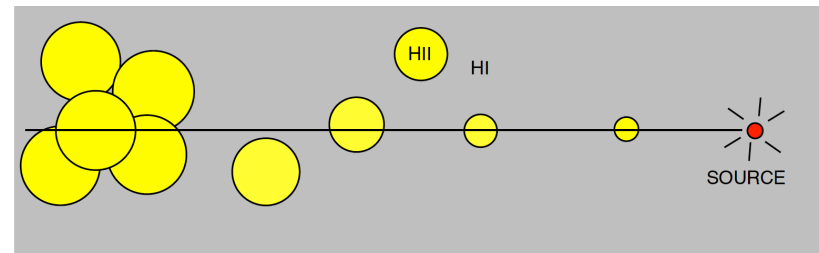
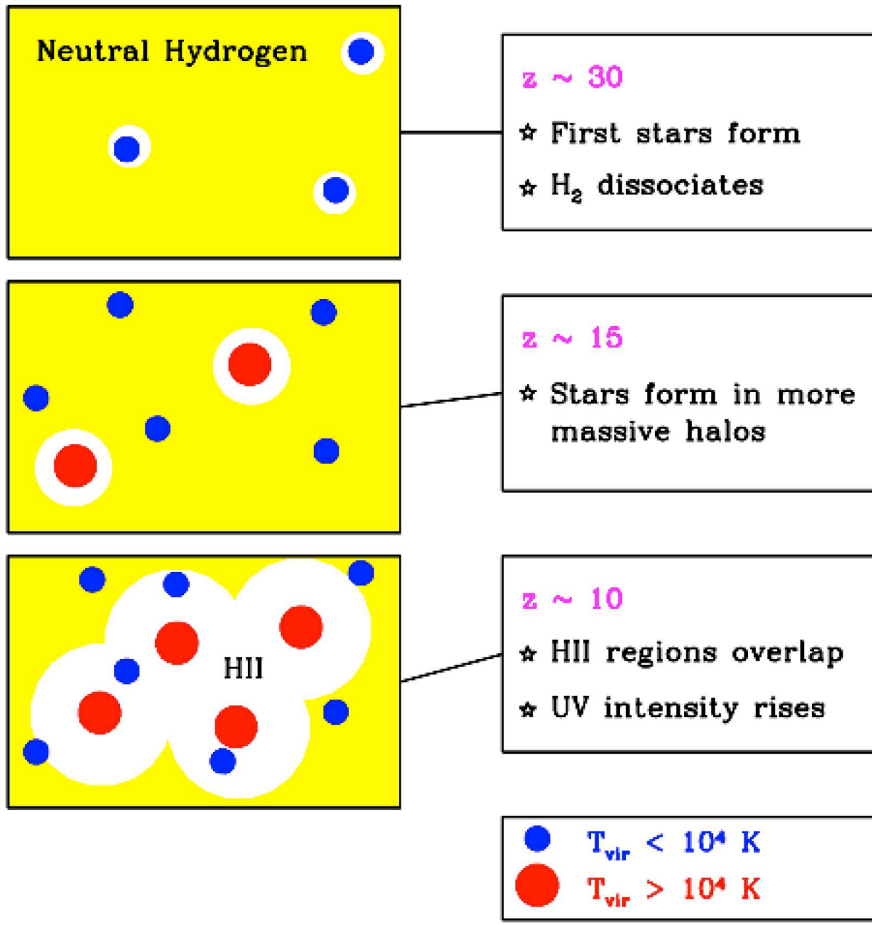
Sponsored by NASA/HST & JWST

Talk is on: http://www.asu.edu/clas/hst/www/jwst/jwsttalks/israel15tau_hstlyc.pdf

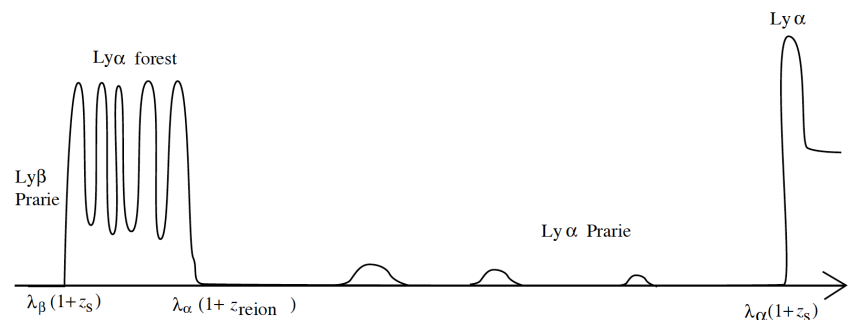


A dim ultraviolet surface brightness is best seen against a dark background.

DETERMINING THE REIONIZATION REDSHIFT



Spectrum



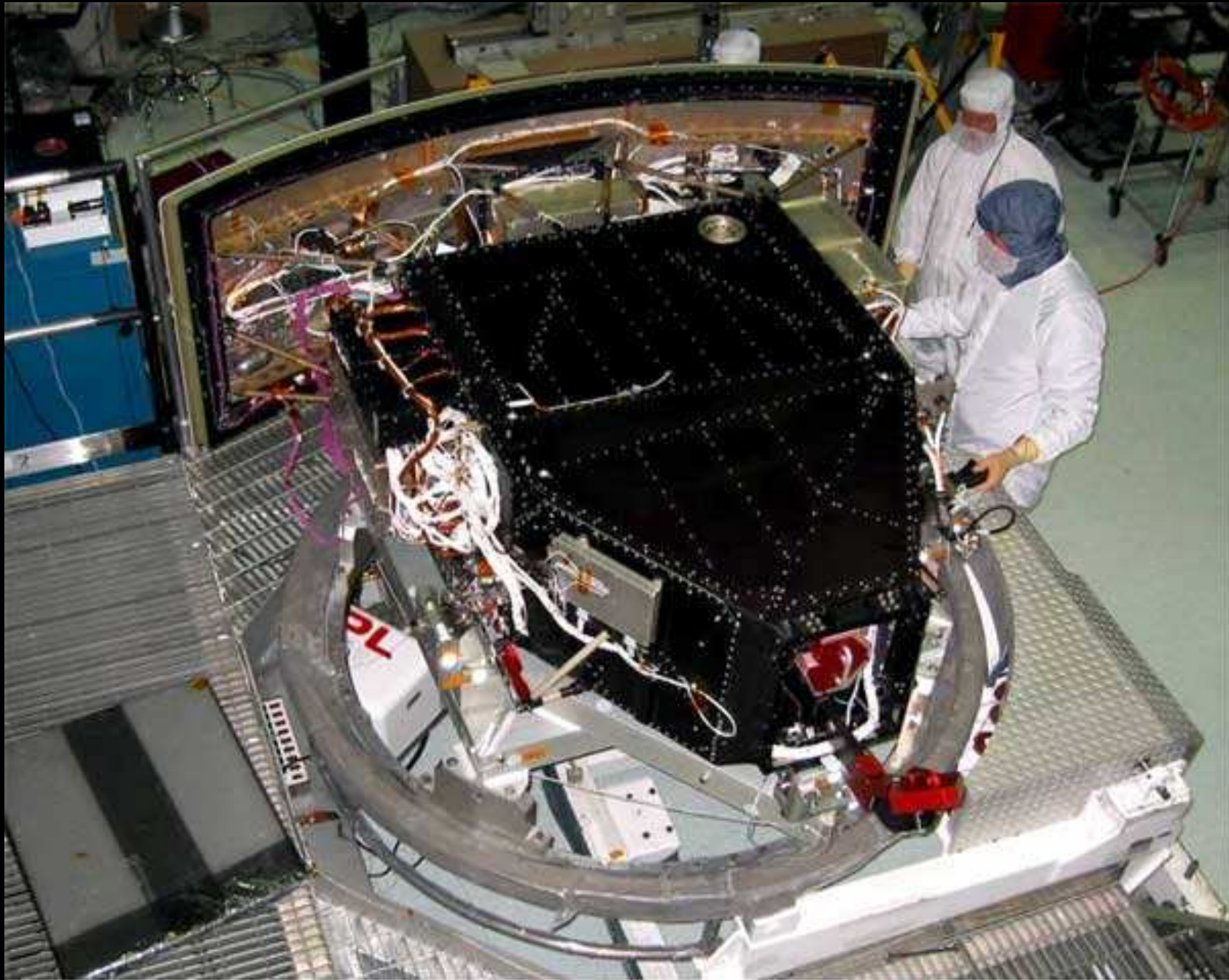
$$1 < \frac{1+z_s}{1+z_{\text{reion}}} < \frac{\lambda_\alpha}{\lambda_\beta} = 1.18$$

Cosmic Reionization (Loeb & Barkana (2001 Ann. Rev. A&A 39, 19):

[LEFT]: Universe reionized when HII-regions from first star-forming galaxies overlap: WMAP9/Planck15: This may have happened at $z \lesssim 8.8 \pm 1.5$.

[RIGHT]: Below a certain redshift ($z \lesssim 5.5$?), IGM is then transparent enough that reionizing Lyman-Continuum (LyC) radiation can reach us.

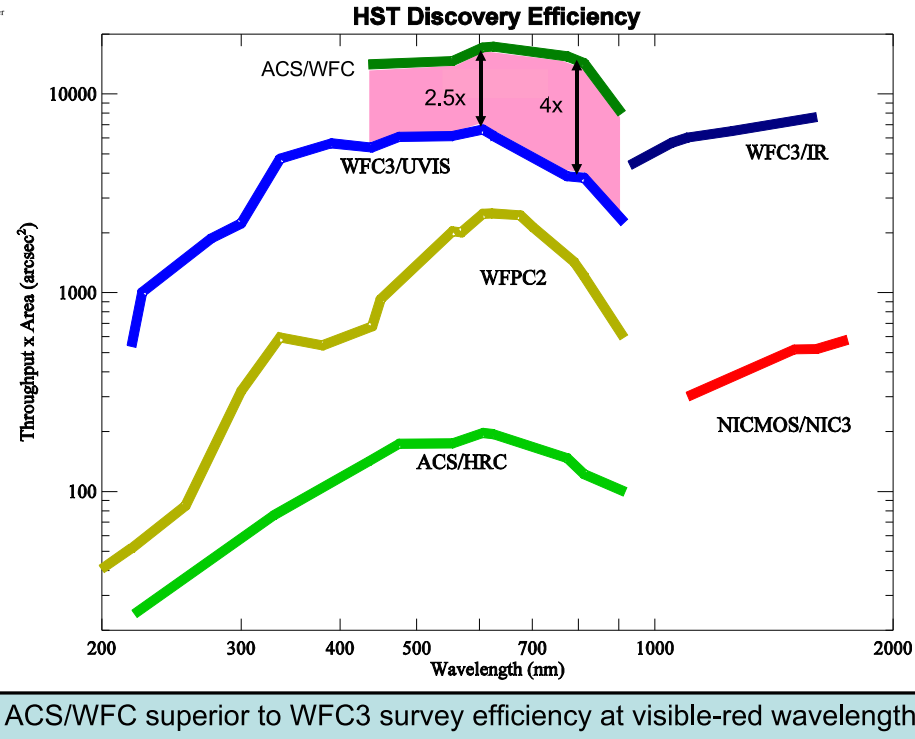
(1a) Hubble Wide Field Camera 3 (WFC3) Data



HST WFC3 and its IR channel: a critical pathfinder for JWST science.



Role of ACS in HST Post-SM4 Imaging Capability



030507_PMB_ACS_Status.ppt

WFC3/UVIS channel unprecedented UV–blue throughput & areal coverage:

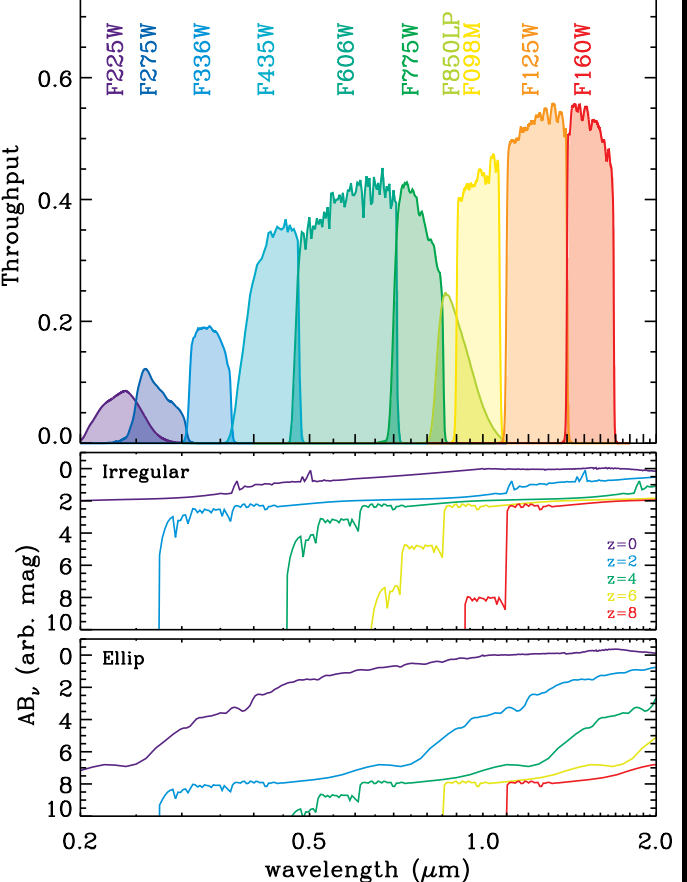
- QE $\gtrsim 70\%$, $4k \times 4k$ array of $0''.04$ pixel, FOV $\simeq 2''.67 \times 2''.67$.

WFC3/IR channel unprecedented near–IR throughput & areal coverage:

- QE $\gtrsim 70\%$, $1k \times 1k$ array of $0''.13$ pixel, FOV $\simeq 2''.25 \times 2''.25$.

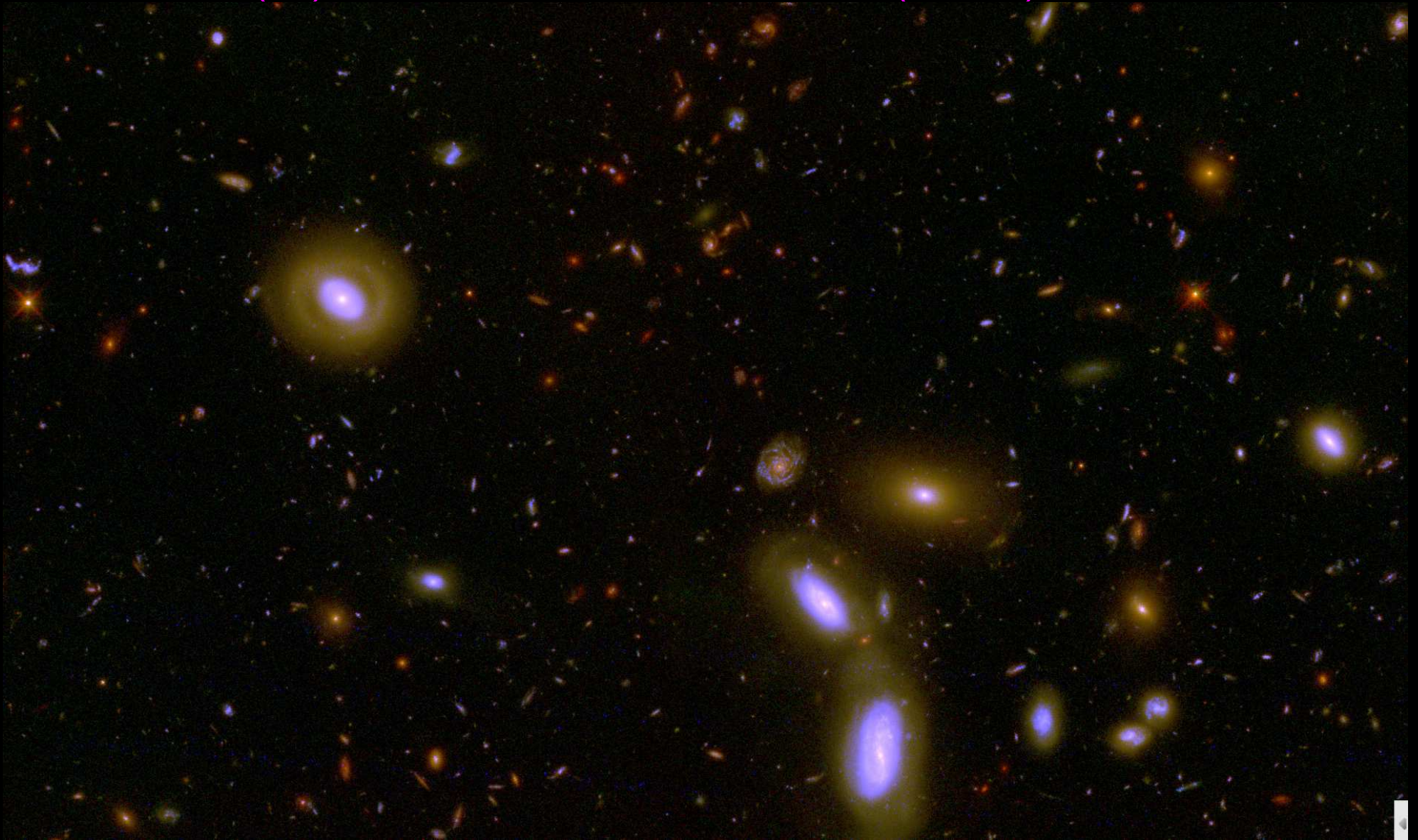
WFC3 filters designed for star-formation and galaxy assembly at $z \simeq 1–8$.

Early Release Science (ERS) field covers 40 arcmin^2 , $0.2–2 \mu\text{m}$ in 10 filters.

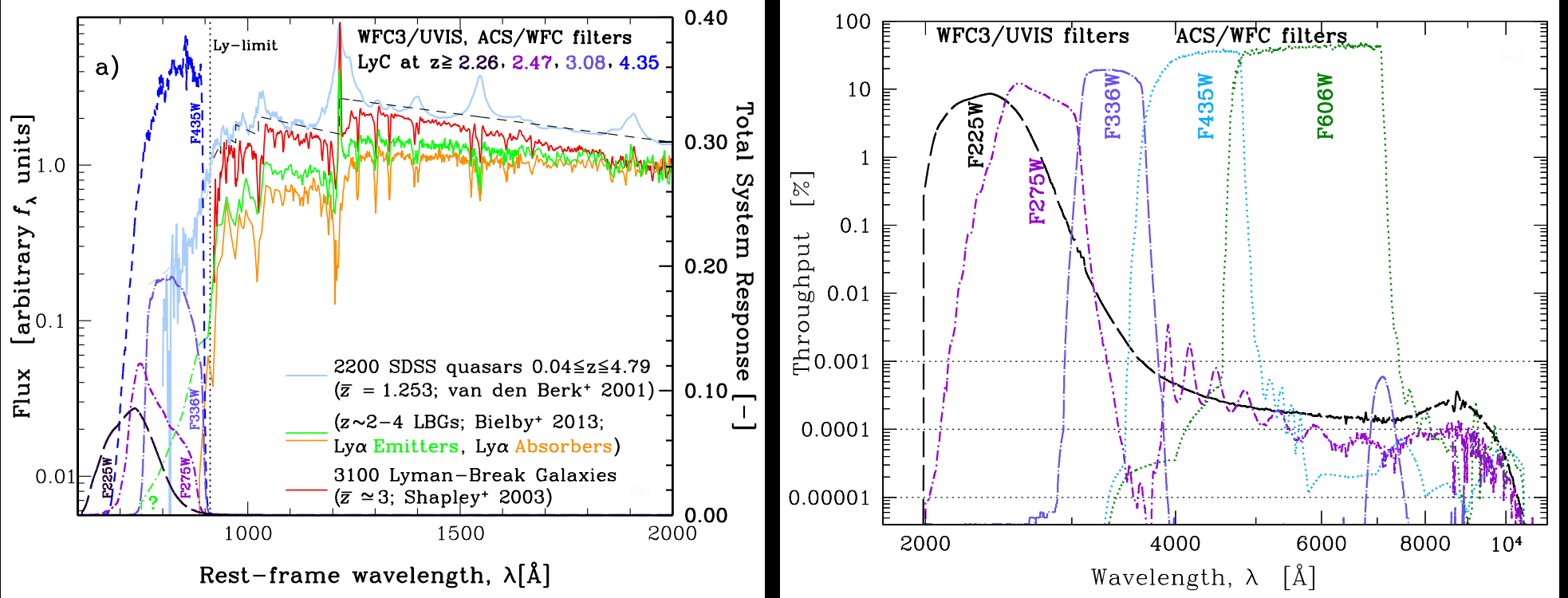


9

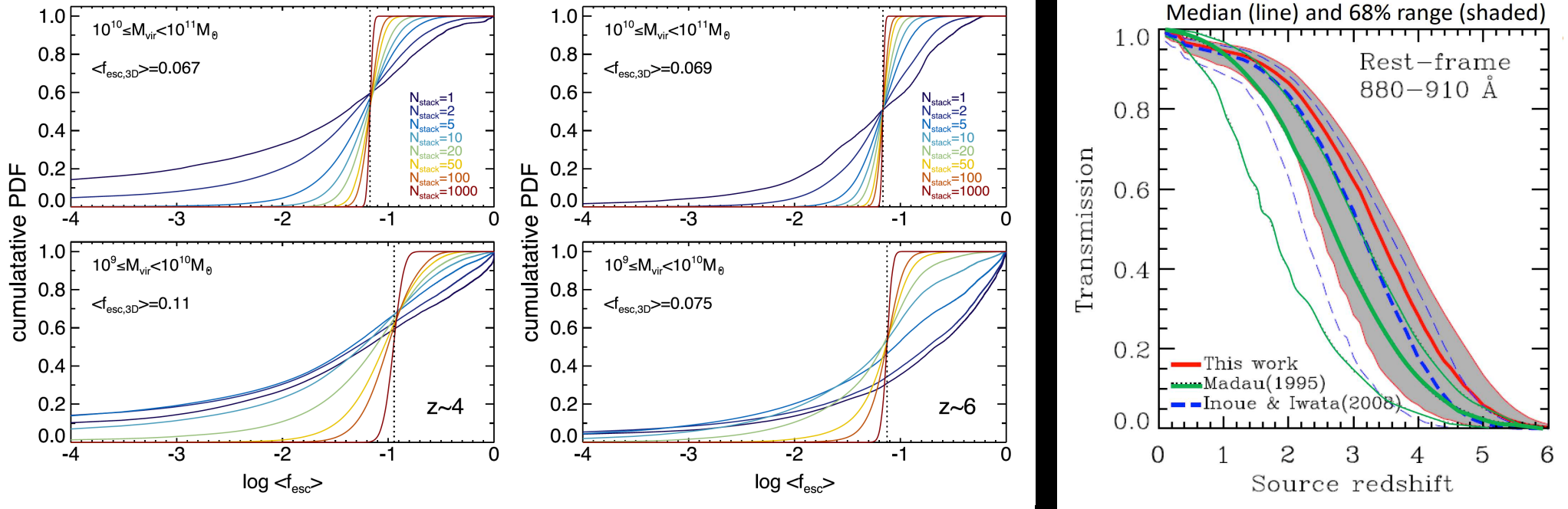
(1a) Hubble Wide Field Camera 3 (WFC3) Data



10 filters with HST/WFC3 & ACS reaching AB=26.5–27.0 mag (10- σ) over 40 arcmin² at 0.07–0.15" FWHM from 0.2–1.7 μ m (UVUBVizYJH). (JWST adds 0.05–0.2" FWHM imaging to AB \simeq 31.5 mag (1 nJy) at 1–5 μ m+ 0.2–1.2" FWHM at 5–29 μ m, tracing young+old SEDs & dust)



- WFC3/UVIS F225W, F275W, F336W, and ACS/WFC F435W filters can capture LyC ($\lambda < 912\text{\AA}$) at $z \geq 2.26$, $z \geq 2.47$, $z \geq 3.08$, and $z \geq 4.35$.
- Lower z -bounds chosen such that *no* $\lambda > 912\text{\AA}$ light is sampled below the filter's red edge (defined at 0.5% of peak transmission).
- Filter red-leak wing ($\lambda \gtrsim 3648\text{\AA}$) is $\lesssim 3 \times 10^{-5}$ of peak transmission.

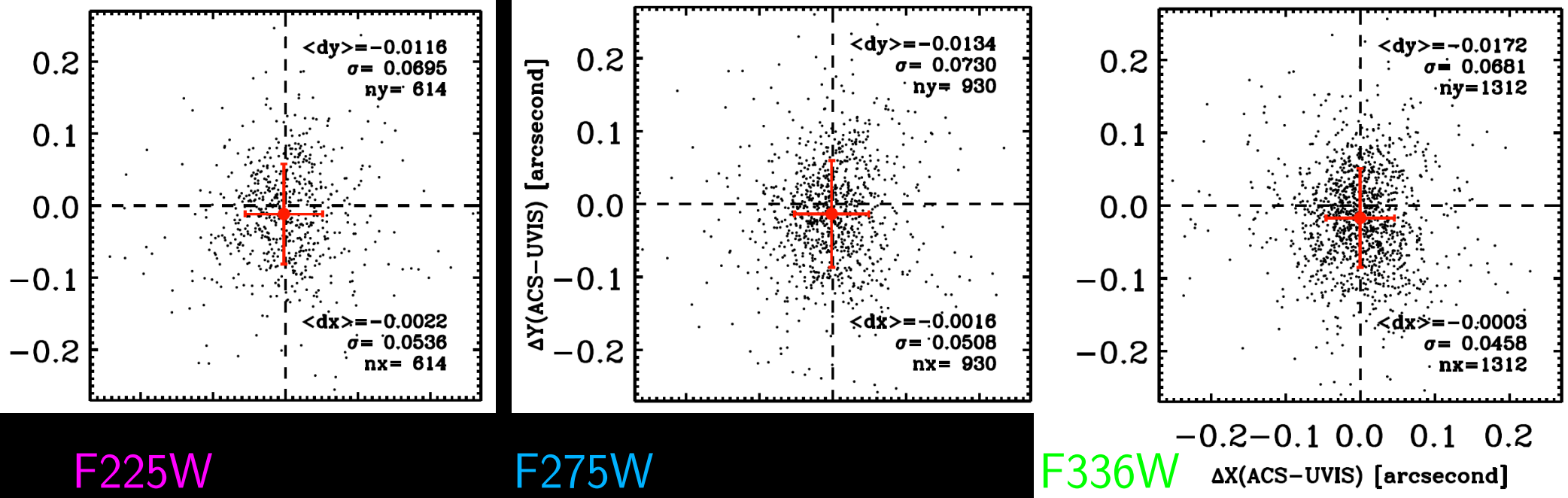


[LEFT] Cen & Kimm (2015): PDFs of mean f_{esc} over “ N_{stack} ” objects: high-mass (top) & low-mass (bottom) at $z=4$ (left) & $z=6$ (right).

- Mean f_{esc} from weighted number of photons mimics SED stacking of galaxy LyC data with true mean f_{esc} listed. ERS has $N_{stack}=11\text{--}37$.

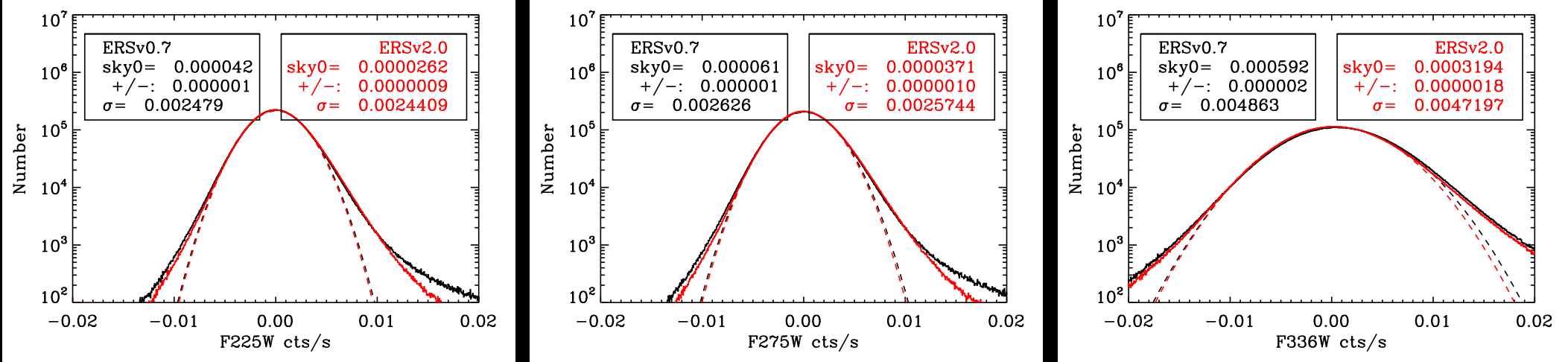
[RIGHT] Inoue et al. (2014, MNRAS 442, 1805): IGM transmission models for f_{esc} calculations: Red is the median and grey the 68% range, based on MC simulations of IGM attenuation vs. z .

Uses updated absorber function + available data on Ly α forest, Damped Lyman Alpha (DLA) & Lyman Limit Systems (LLS) mean-free paths.



The first, hardest part was to get the WFC3 astrometry right:

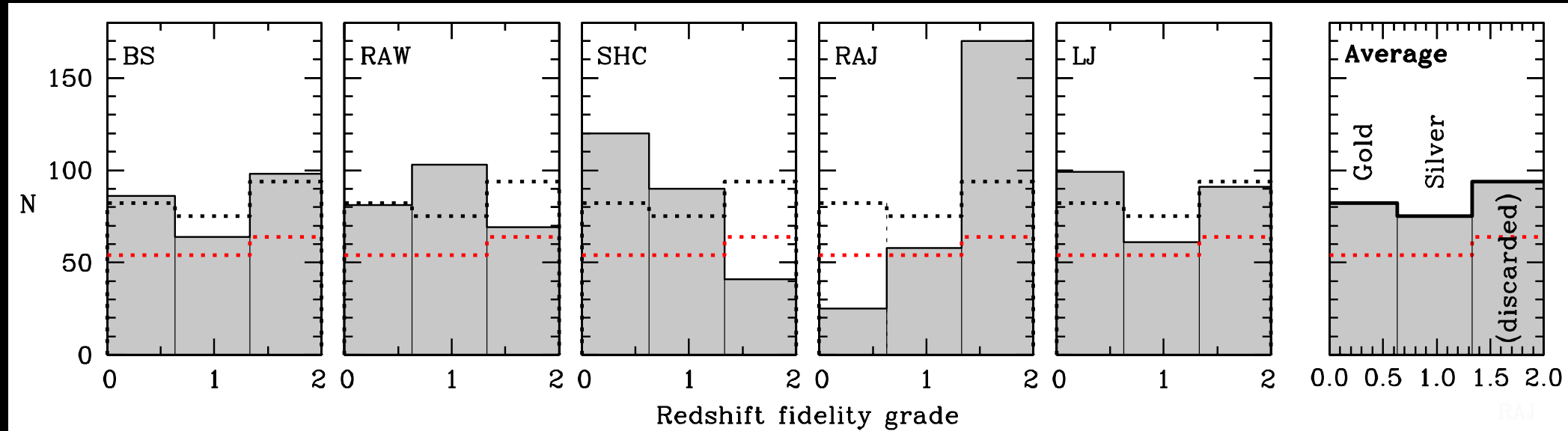
- Pre-flight 2009 ERS geo-distortion had $\lesssim 0\text{!}'45$ offsets at image borders compared to GOODS v2.0 (Windhorst et al. 2011 ApJS, 193, 27).
- In-flight 2013 geo-distortion correction yielded excellent registration of all WFC3/UVIS tiles to the ACS F435W mosaics (Kozhurina et al. 2013).
- Compared to GOODS, all offsets are now $\lesssim 0\text{!}'02 \pm 0.06$ (rms) in all LyC filters (Smith et al. 2015) — this no longer blurs any LyC signal!
- Any LyC signal can now be measured and stacked, including removal of all foreground interlopers ($AB \lesssim 27.5$), and measurement of LyC light-profiles.



Residual sky-background levels in the drizzled WFC3/UVIS ERS mosaics:

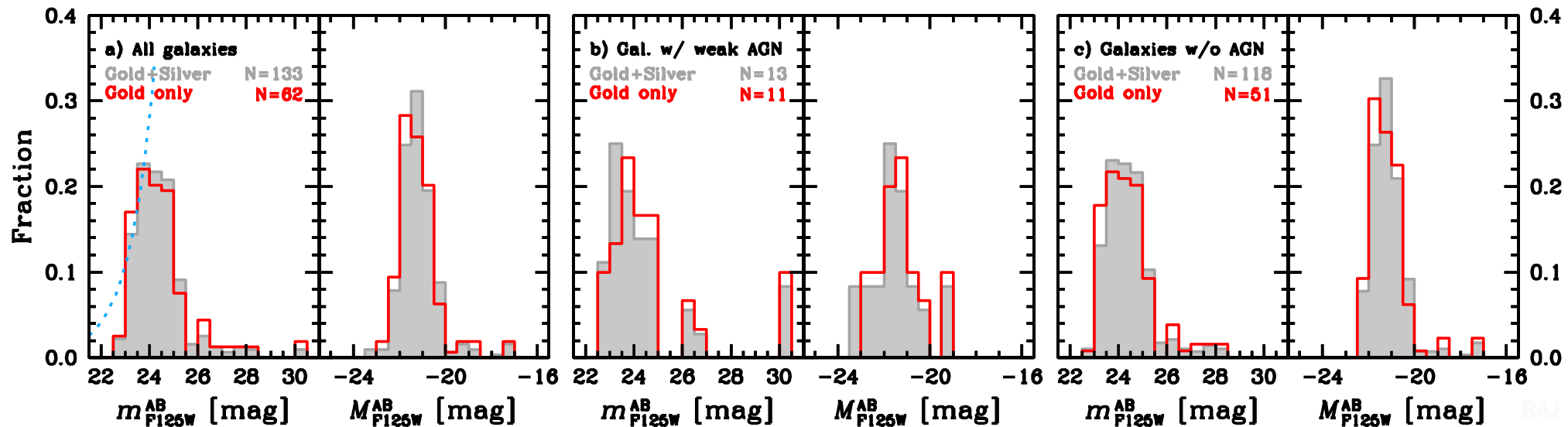
- Black lines: best fit to the 2009 ERS v0.7 mosaics of Windhorst et al. (2011), which used pre-flight thermal vacuum flat-fields.
- Red lines: current mosaics (ERS v2.0; Smith et al. 2015), using best available on-orbit calibrations.
- Global *residual sky-background levels (in ADU/sec)* remaining after drizzling the ERS mosaics are ~ 30.29 , 29.99 , and $28.15 \text{ mag arcsec}^{-2}$.
- These are removed in three stages: globally during drizzling ($\text{Zodi} \simeq 25.5 \text{ mag arcsec}^{-2}$), locally before stacking, and again locally after stacking (to do the photometry). This is absolutely critical for optimal LyC stacking.
- Final 71×71 pix ($6'!39 \times 6'!39$) LyC stacks allow *residual* local sky-subtraction to $\lesssim 32.3 \text{ mag arcsec}^{-2}$.

(1b) Hubble WFC3 ERS — Spectroscopic Sample Selection



Comparison of redshift reliability (spectrum quality) assessments, from best (0.0) to poorest (2.0), by five co-authors [BS, RAW, SHC, RAJ, and LJ]:

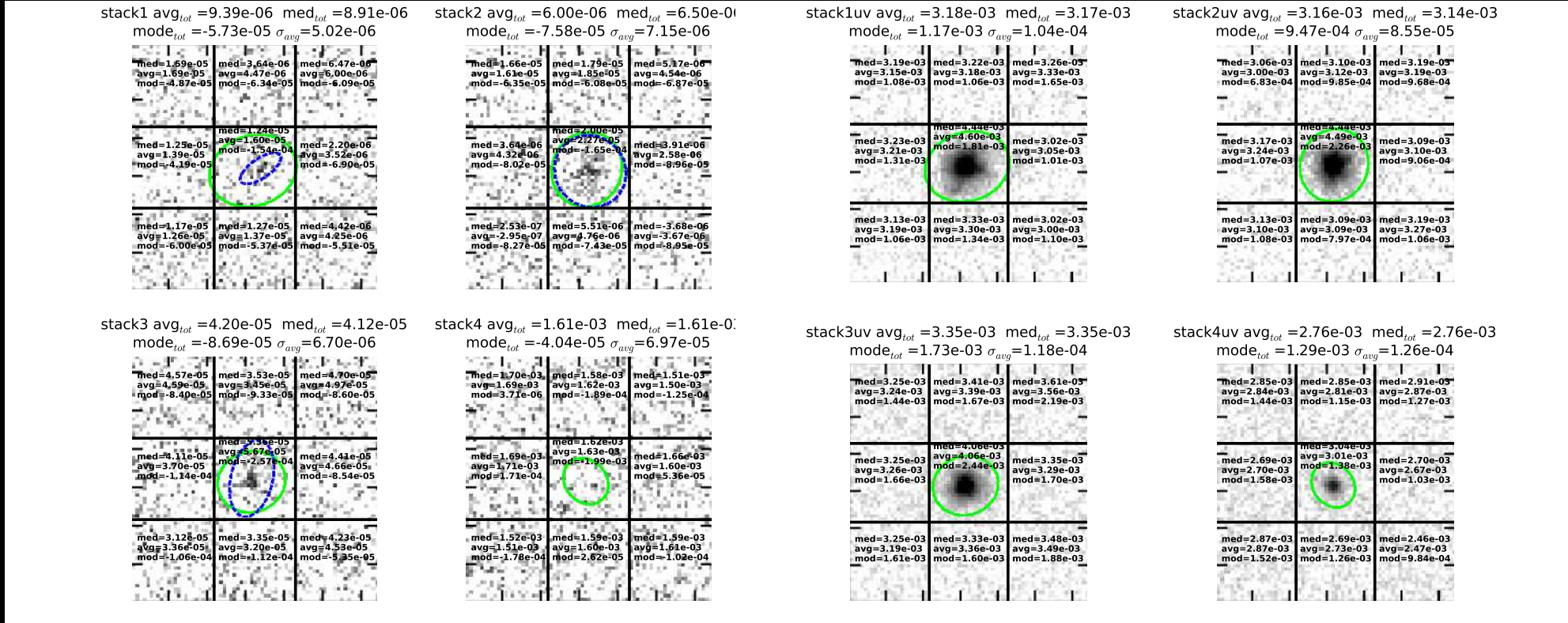
- Measuring LyC escape fractions of $f_{esc} \simeq 6.0\%$ at $\gtrsim 3\sigma$ requires low interloper fraction (Siana⁺ 2015; Vanzella⁺ 2015).
- Mask-out all interlopers from 10-band ERS mosaics to AB $\lesssim 27.5$ mag.
- Use all VLT, Keck, & HST grism spectra to get most reliable samples:
- “Gold” sample: highest fidelity (grades=0–0.63): spec-z’s very likely correct.
- “Silver” sample: next highest fidelity (0.64–1.33), with z’s likely correct.



Absolute and apparent WFC3/IR F125W (J -band) magnitude distributions of the Gold and combined Gold + Silver samples:

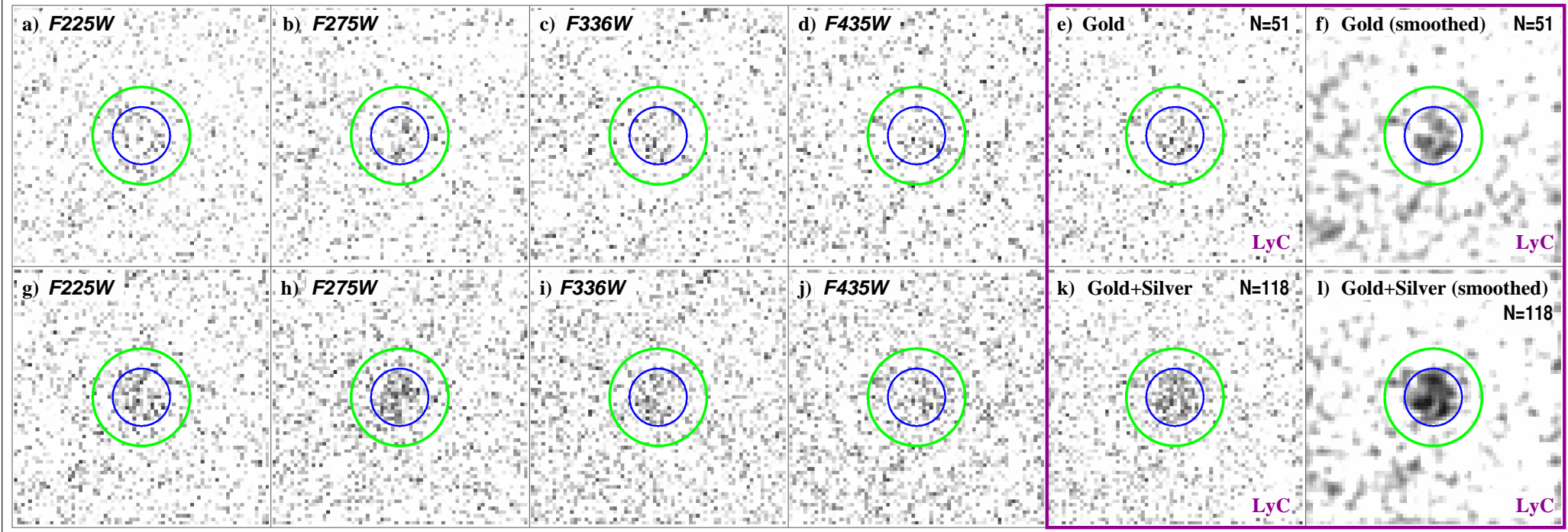
- The F125W filter samples rest-frame near-UV emission at $2.26 \lesssim z \lesssim 5$. It serves as a proxy for restframe M_{AB} (1650Å) for flat spectrum objects.
- The blue dotted curve indicates the faint-end power-law slope of 0.16 dex/mag of the galaxy number counts of W11.
- Sample incompleteness for $AB \gtrsim 24$, or M_{AB} (1650) $\gtrsim -21$ mag.
- Any LyC AB-fluxes & f_{esc} -values are only valid for these luminosities!

• (2) WFC3 & ACS Lyman Continuum Stacking, Systematics, & Fluxes



“Tic-tac-toe” sky-background analysis of 71×71 pixel ($6!39 \times 6!39$) stacks:
LyC [*left 4 panels*] and UVC [*right 4 panels*].

- Large-scale gradients in residual sky-background left in drizzled images are $5\text{--}40\times$ fainter than the *global* remaining sky residuals in previous Fig.
- Residual sky-gradients on 71×71 pixel scales are fainter than ~ 32.3 mag arcsec $^{-2}$ across the “tic-tac-toe” apertures. This is fainter than the LyC SB-signal where this can be measured, but does constitute a (fundamental?) limit to how many images can be stacked.

Galaxies without AGN, $2.3 \lesssim z \lesssim 6$  $z=2.26-2.47$ $z=2.47-3.08$ $z=3.08-4.35$ $z=4.35-6$ WEIGHTED ALL: $z=2.26-6$.

[*Top Row*]: All galaxies in combined Gold Galaxy sample: $N=51$;

[*Bottom Row*]: All galaxies in combined Gold+Silver sample: $N=118$.

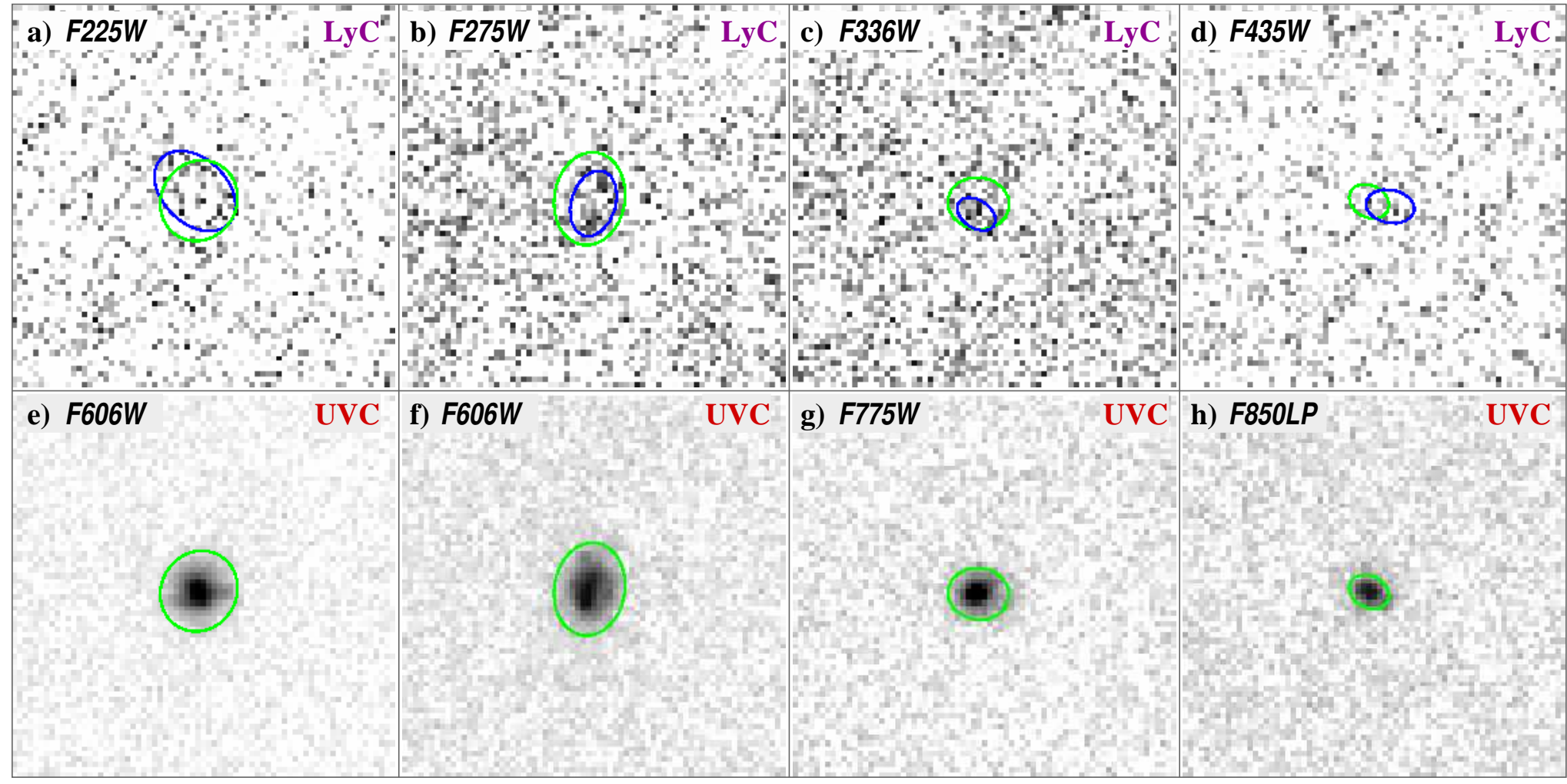
[*Right 2×2 panels*]: Weighted “stack-of-stacks” over all 4 LyC filters: best visualizes LyC of galaxies at $z \simeq 2.3-5.5$. Formal detection S/N -ratios:

$\gtrsim 6.8\sigma$ ($\sim \sqrt{51} \times 1.0\sigma$ above sky), and $\gtrsim 13\sigma$ ($\sim \sqrt{118} \times 1.2\sigma$).

Equivalent to 22–236 orbit stacks with HST, respectively!

Circles: $r=8$ ($0\text{!}72$), 13 pix ($1\text{!}17$), centered on the UVC emission.

Galaxies without AGN, Gold sample



$z=2.26-2.47$

$z=2.47-3.08$

$z=3.08-4.35$

$z=4.35-6.$

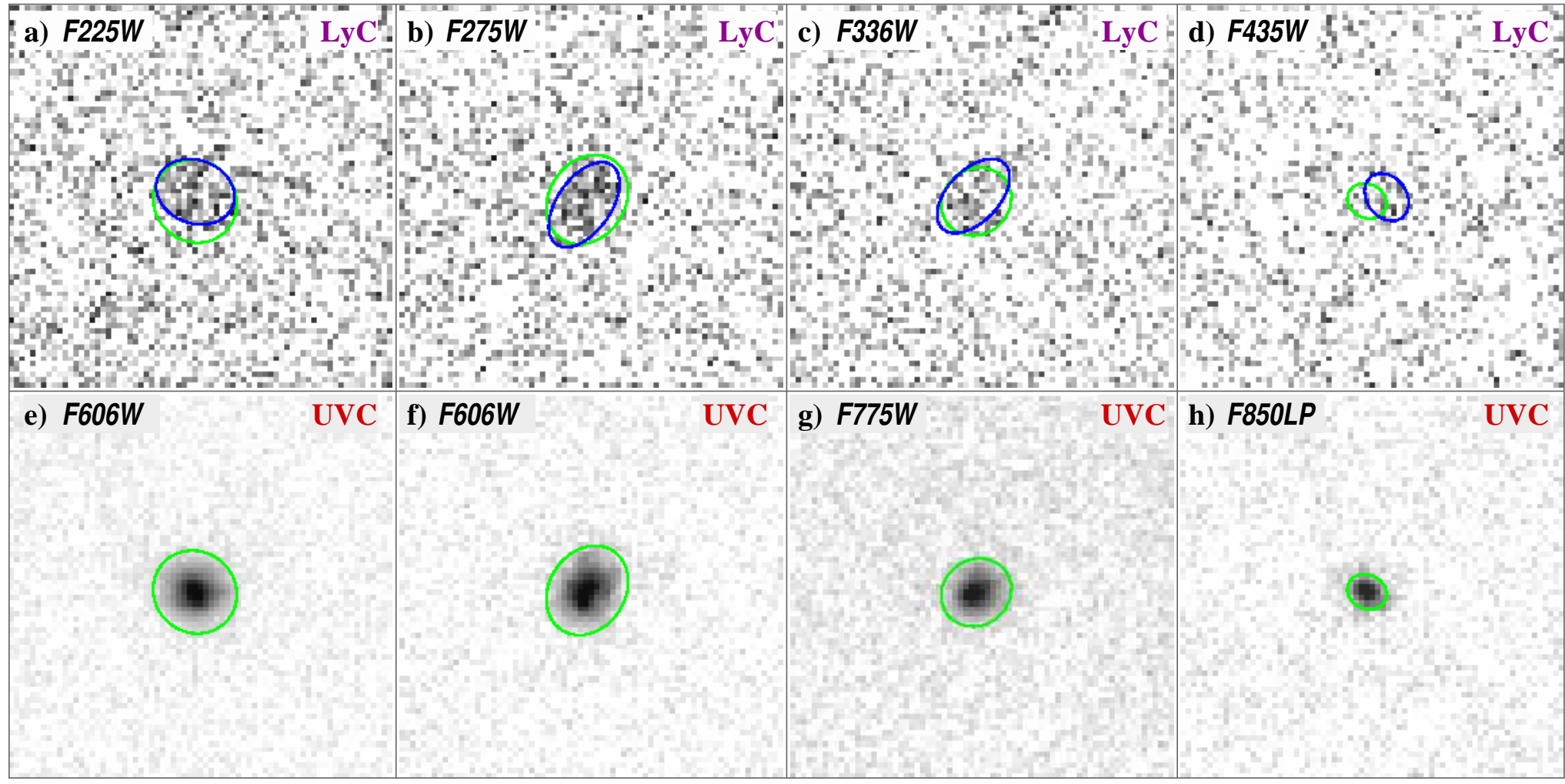
Galaxies without AGN in Gold sample.

Top row: Ly-Continuum stacks, Bottom Row: UV-Continuum stacks.

Blue: SExtractor LyC apertures, $\gtrsim 1\sigma$ in $\gtrsim 4$ connected pixels.

Green: SExtractor MAG_AUTO apertures using UVC centroids+apertures.

Galaxies without AGN, Gold+Silver sample



$z=2.26-2.47$

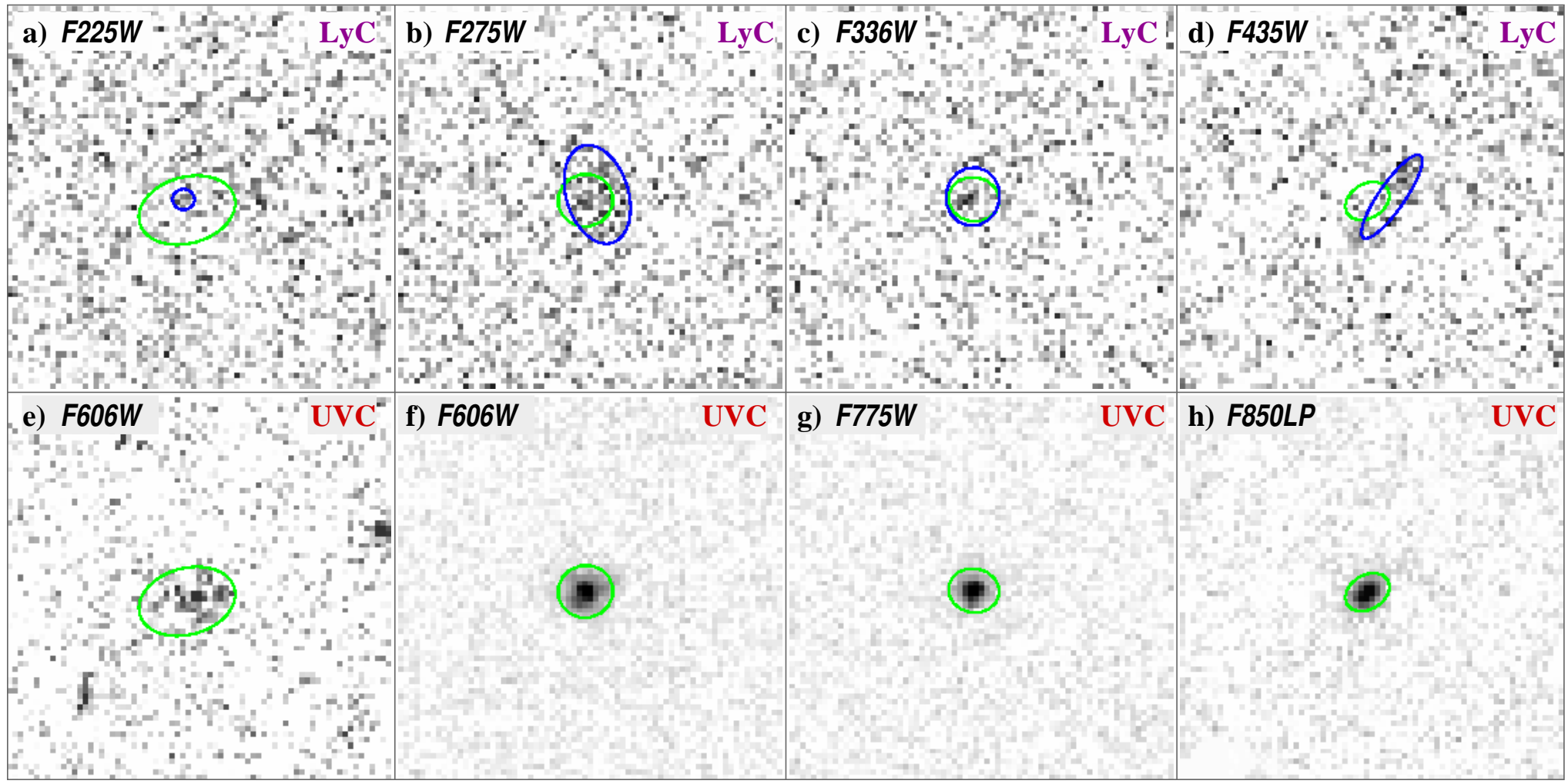
$z=2.47-3.08$

$z=3.08-4.35$

$z=4.35-6.$

Galaxies without AGN in combined Gold + Silver sample.

Galaxies with AGN, Gold sample



$z=2.26\text{--}2.47$

$z=2.47\text{--}3.08$

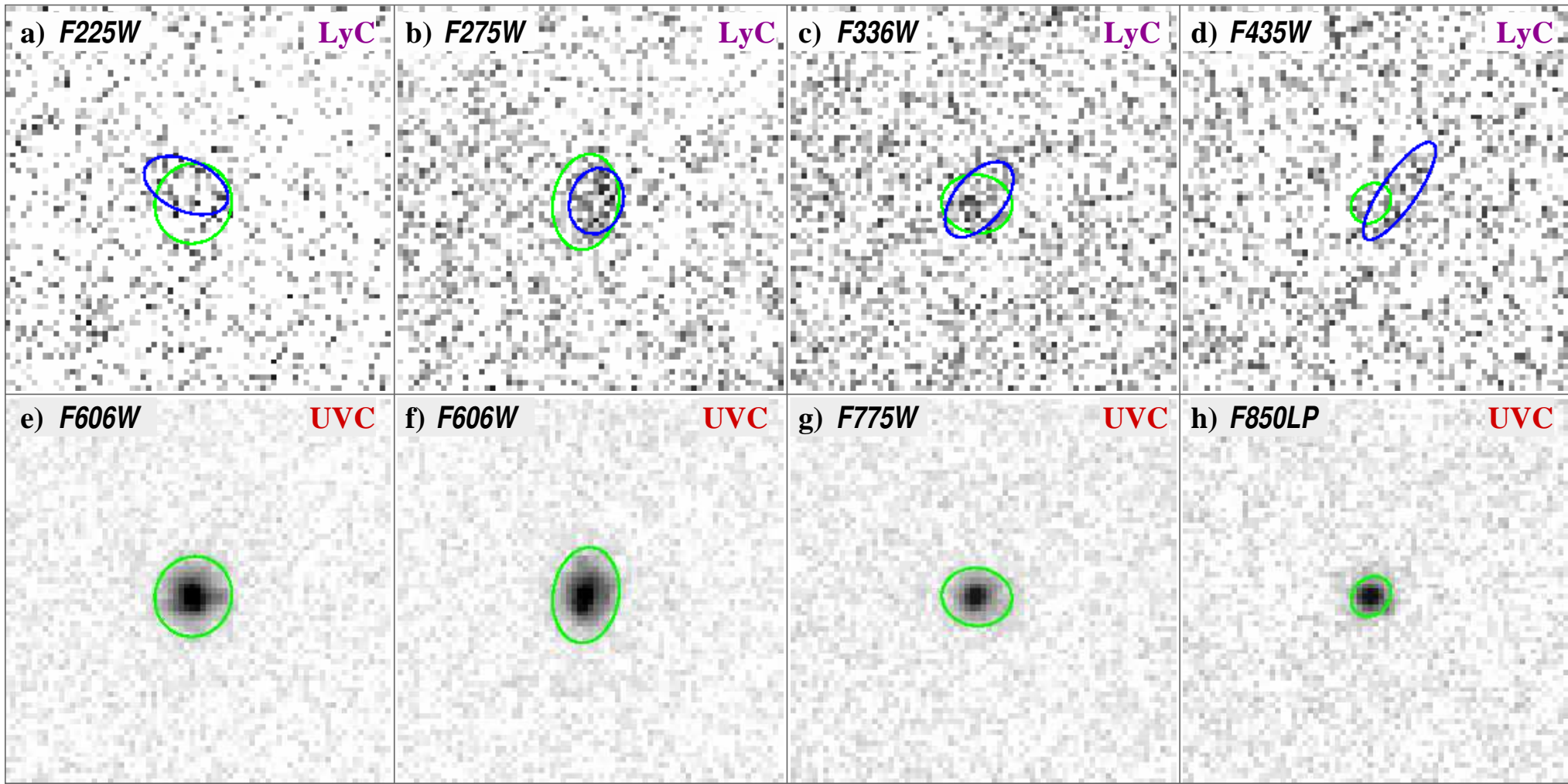
$z=3.08\text{--}4.35$

$z=4.35\text{--}6.$

Galaxies hosting weak AGN in Gold sample.

[Lower Left]: N=1 AGN with background objects shown before masking-out.

All galaxies, Gold sample



$z=2.26-2.47$

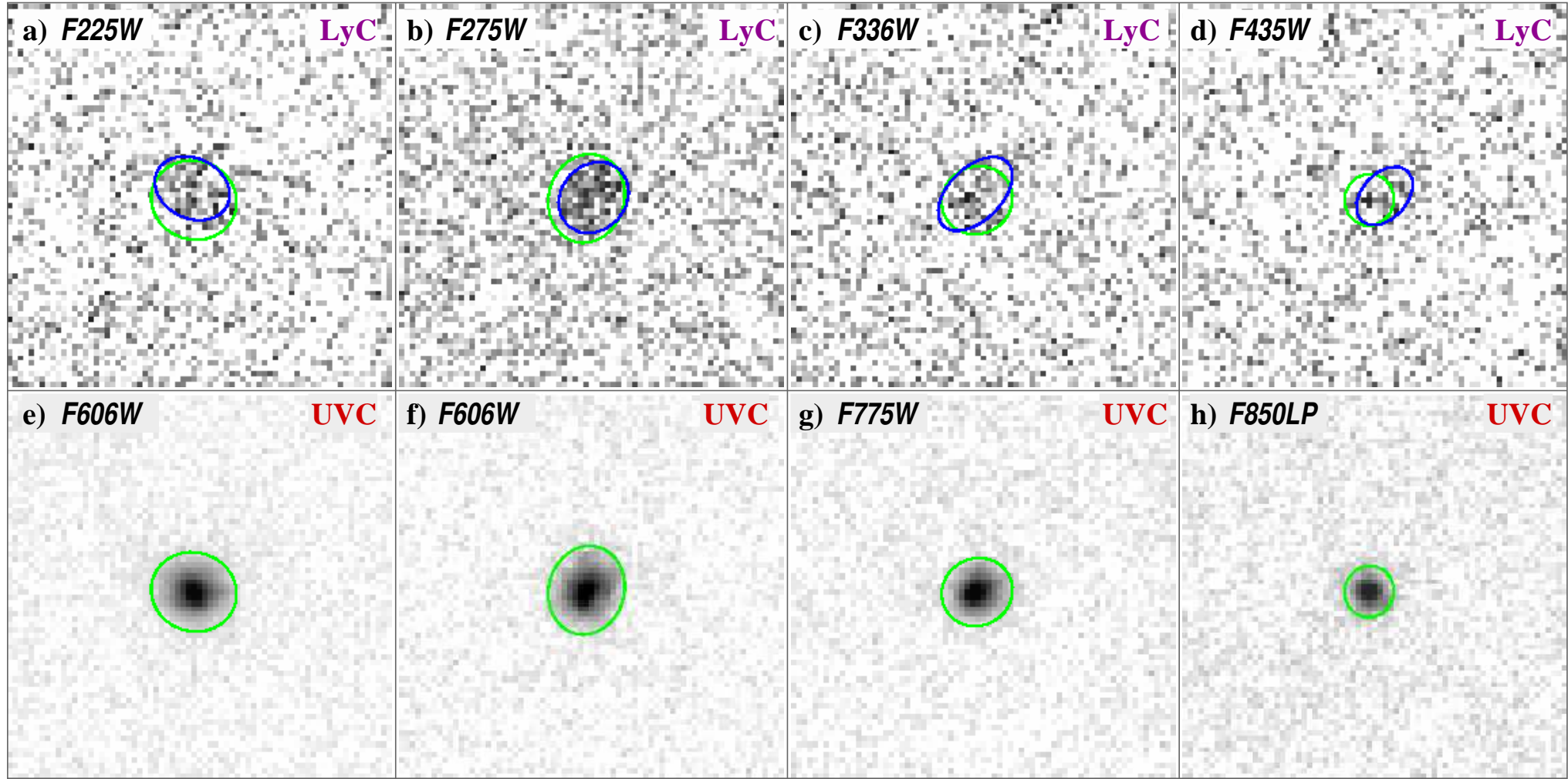
$z=2.47-3.08$

$z=3.08-4.35$

$z=4.35-6.$

All Objects (Galaxies + Weak AGN) in Gold sample.

All Galaxies, Gold+Silver sample



$z=2.26-2.47$

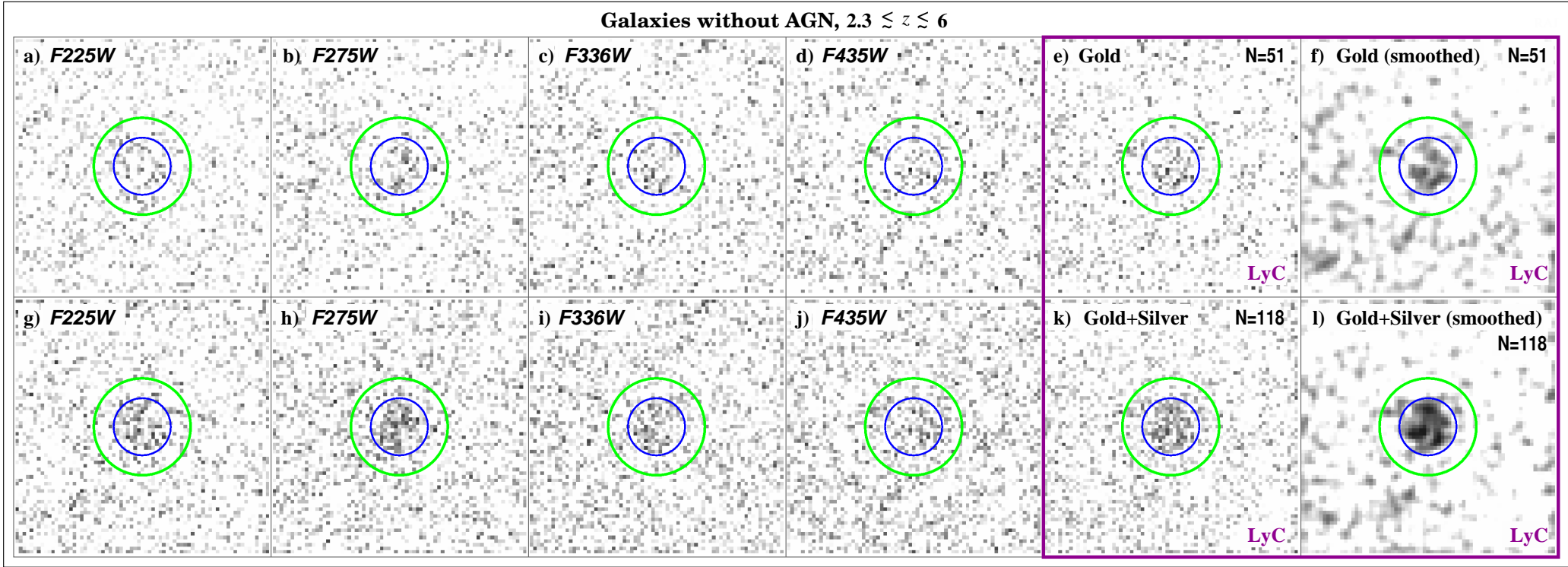
$z=2.47-3.08$

$z=3.08-4.35$

$z=4.35-6.$

All Objects (Galaxies + Weak AGN) in Gold+Silver sample.

- (3) Stacked UV and Lyman Continuum Light-Profiles



$z=2.26-2.47$

$z=2.47-3.08$

$z=3.08-4.35$

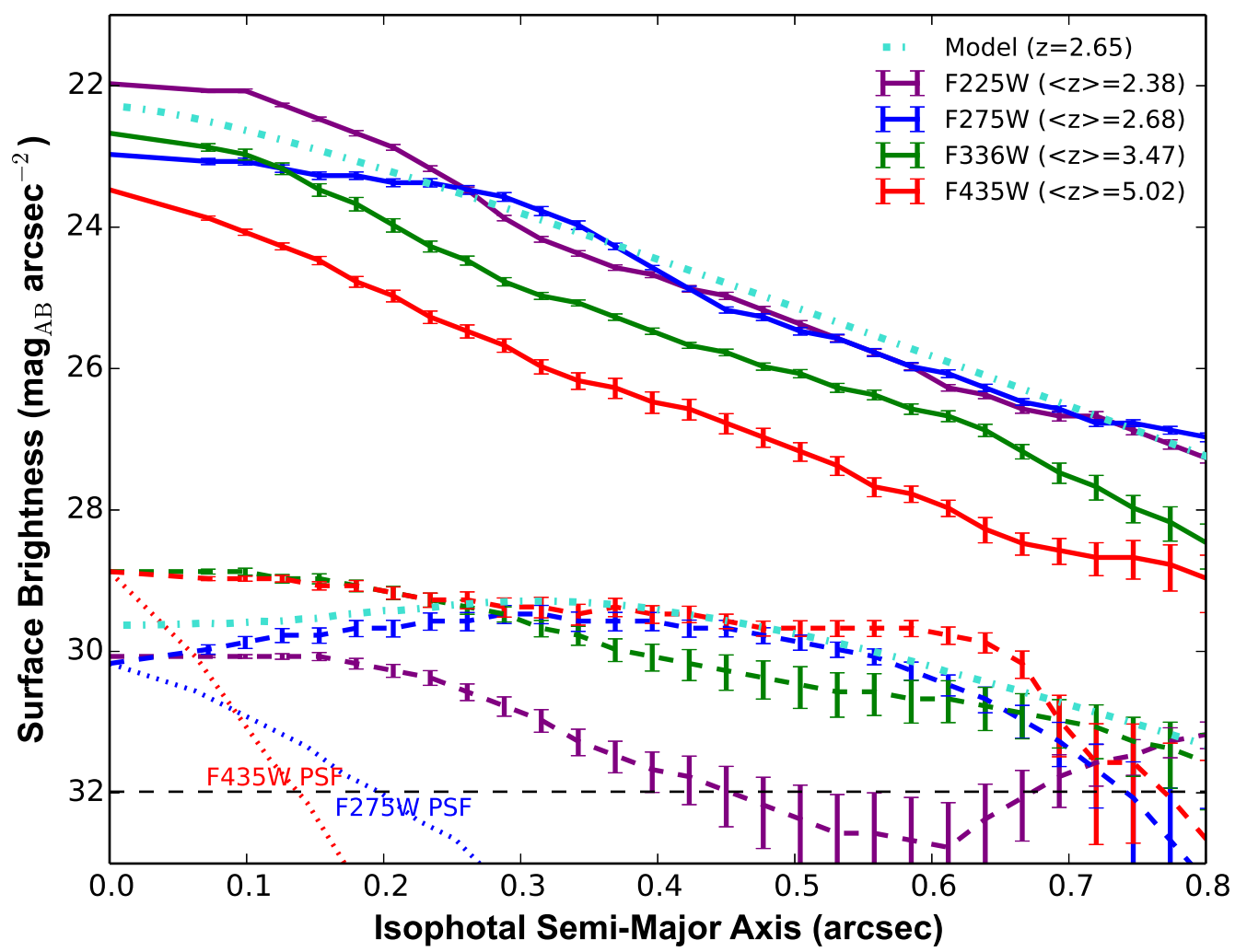
$z=4.35-6$

WEIGHTED ALL: $z=2.26-6$.

[*Top Row*]: All galaxies in combined Gold Galaxy sample: $N=51$;

[*Bottom Row*]: All galaxies in combined Gold+Silver sample: $N=118$.

- The faint LyC emission has a very flat SB-distribution with radius:
- *On average escapes along few random sight-lines through a porous ISM?*
- Not centrally concentrated with few clear sight-lines per galaxy.
- Likeliest escape paths may be somewhat offset from galaxy center.



[Top Curves]: Radial SB-profiles of non-ionizing UVC (*solid*).

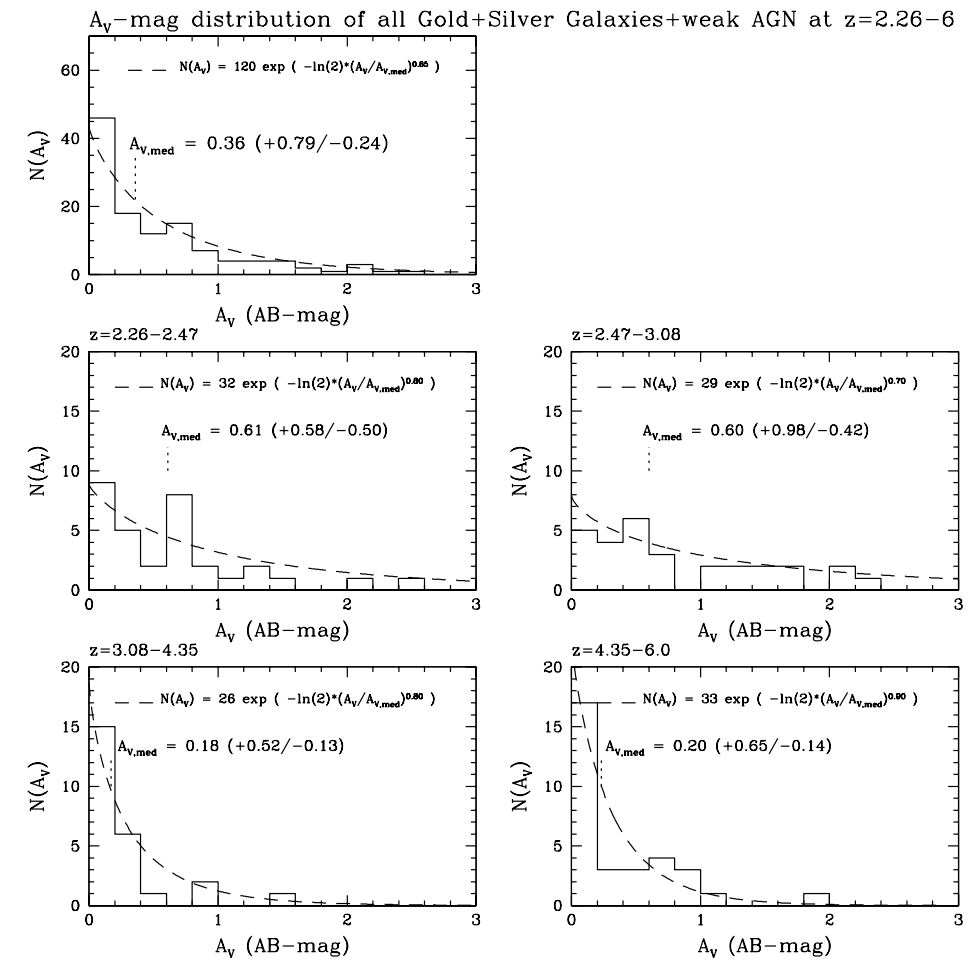
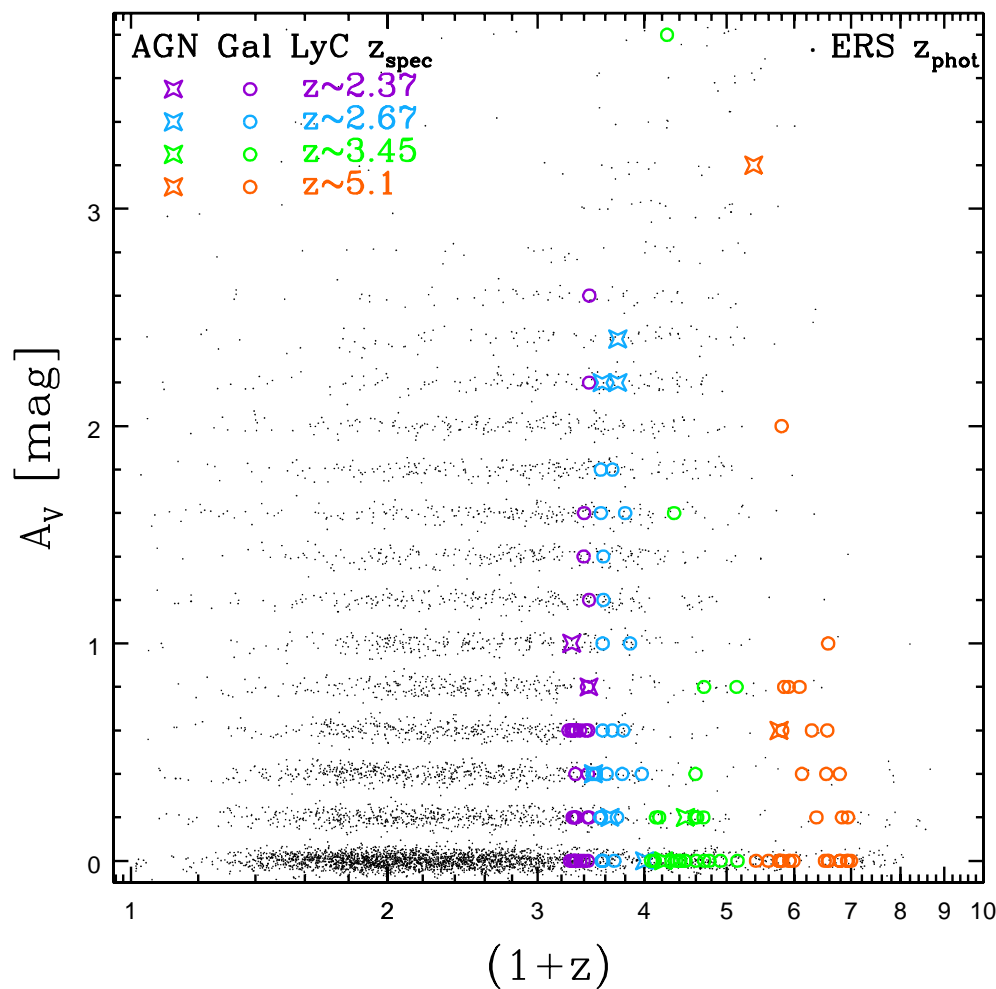
[Bottom Curves]: Radial SB-profiles of LyC signal (*dashed*):

- All LyC SB-profiles are extended compared to the PSFs (dotted).

Horizontal black dashed line is the 1σ SB-limit of ~ 32 mag arcsec⁻².

Light-blue dot-dashes is $z=2.68$ UVC-scattering model with ISM porosity and escaping LyC increasing as: $f_{\text{cov}}(r) = \mathcal{N} \exp\{-(r/10 \text{ kpc})^x\}$.

● (4) Spectral Energy Distribution (SED)-fitting & Dust (A_V) -distribution

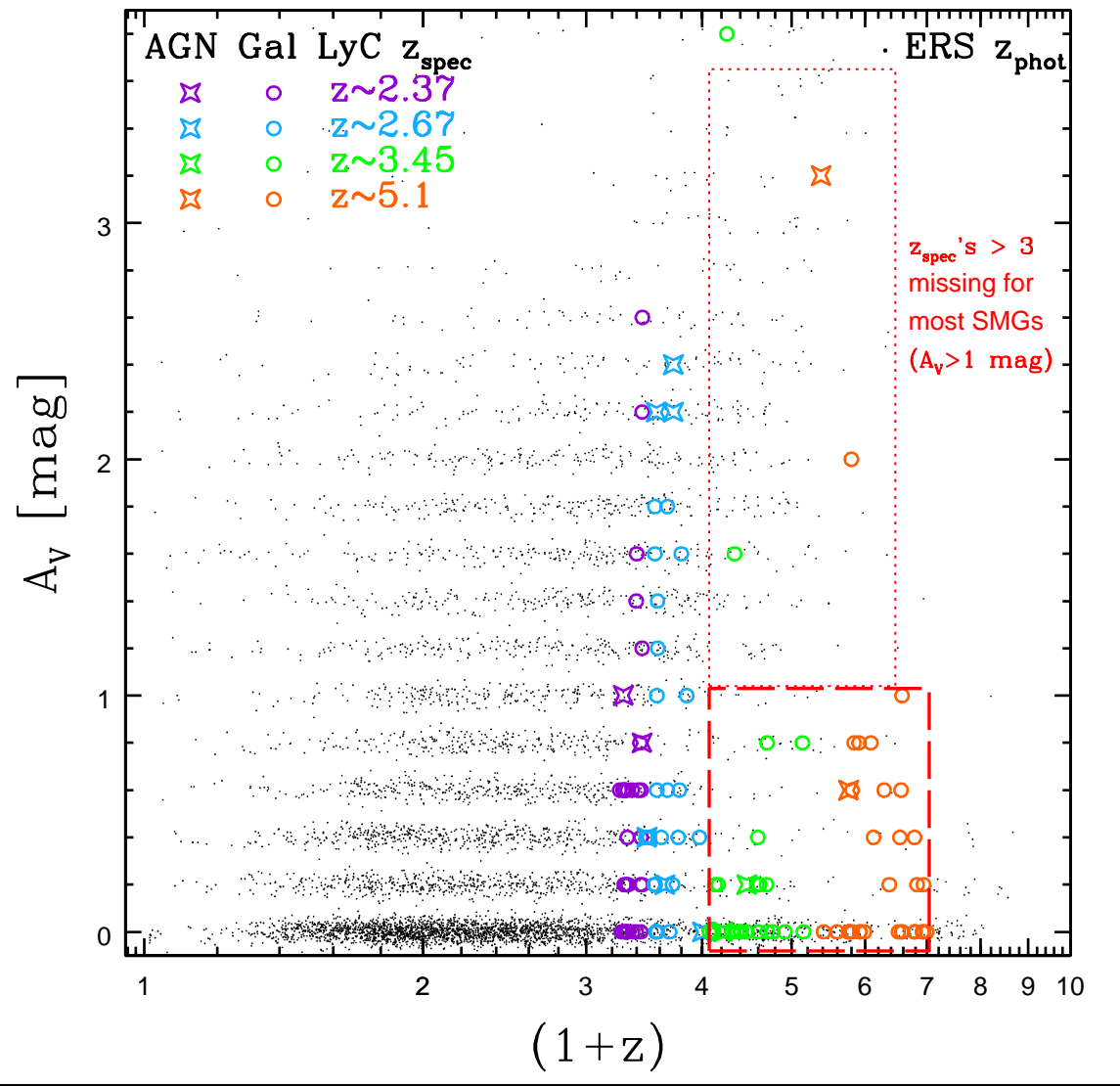


[LEFT]: Best-fit A_V from 10-band SEDs for all ERS galaxies (black dots).

Circles: galaxies; Asterisks: AGN at: $z=2.37$, $z=2.68$, $z=3.45$, $z=5.1$.

[RIGHT]: Adopted distributions $N(A_V)$ for total Gold + Silver LyC sample (top), and for each of the four redshift bins:

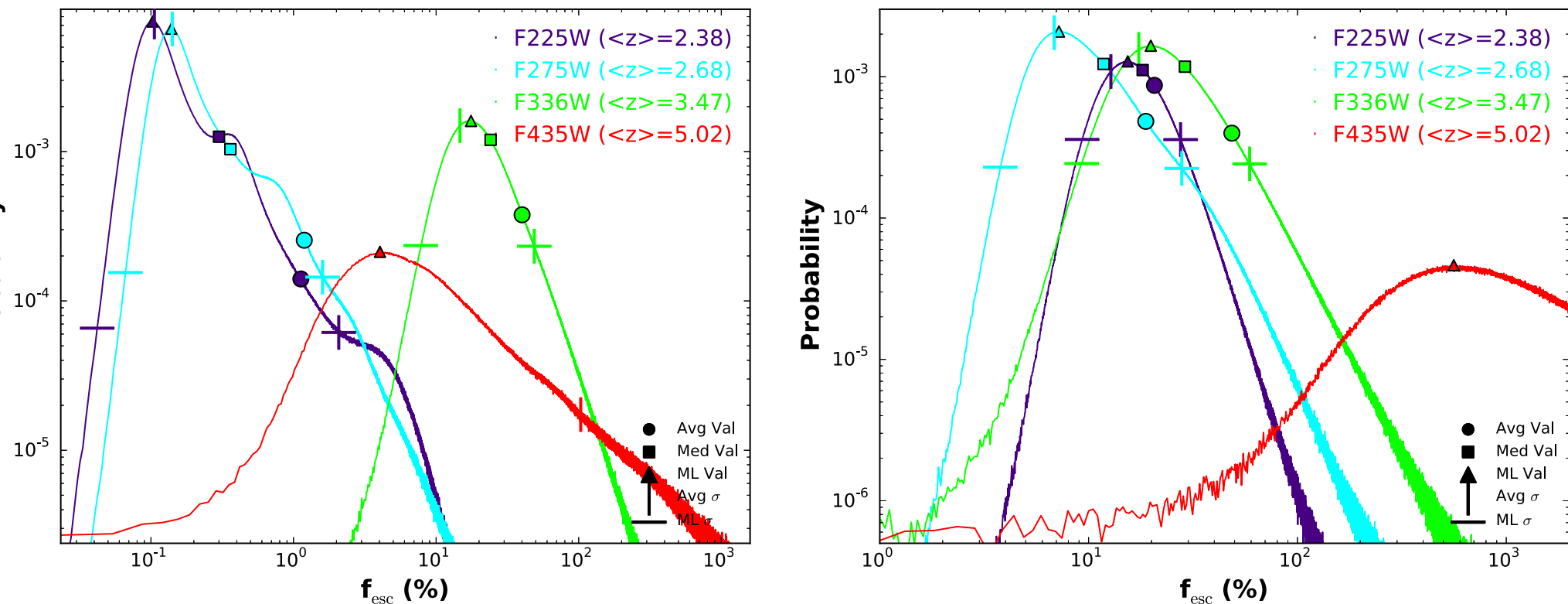
Median A_V increases from ~ 0.2 at $z=5.1-3.5$ to ~ 0.6 at $z=2.67-2.37$.



Best-fit A_V from 10-band SEDs for all ERS galaxies (black dots).

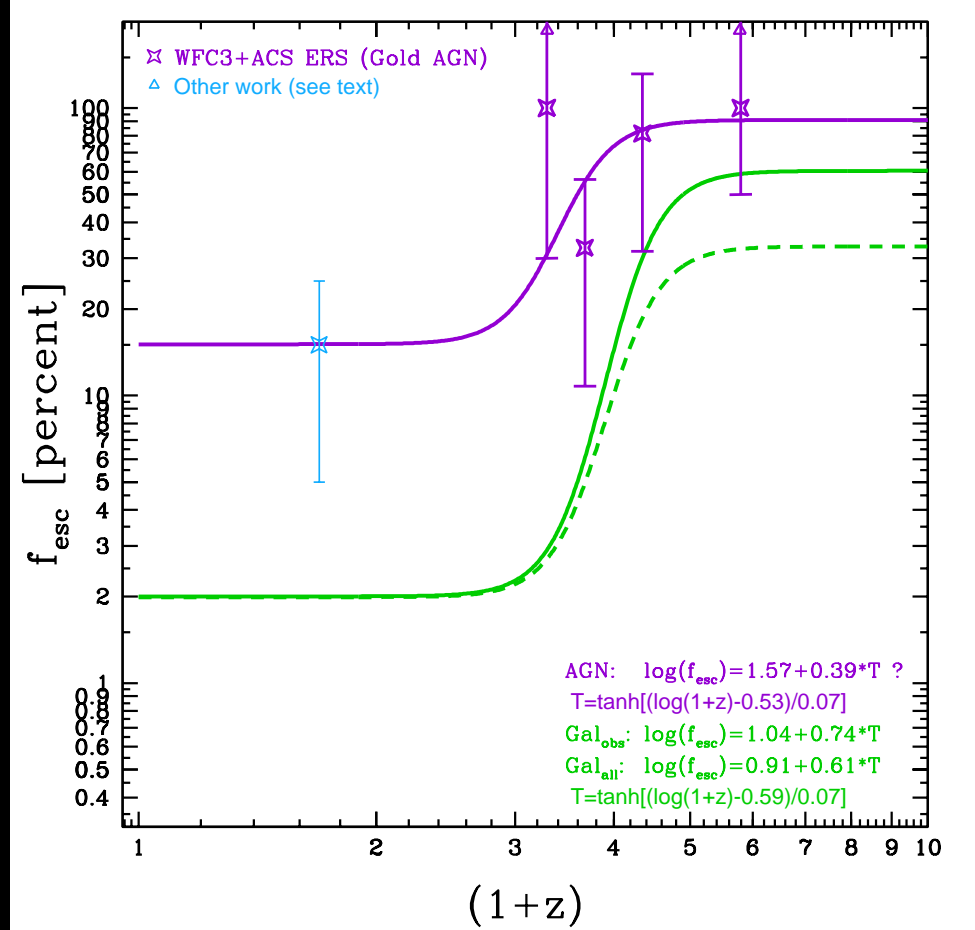
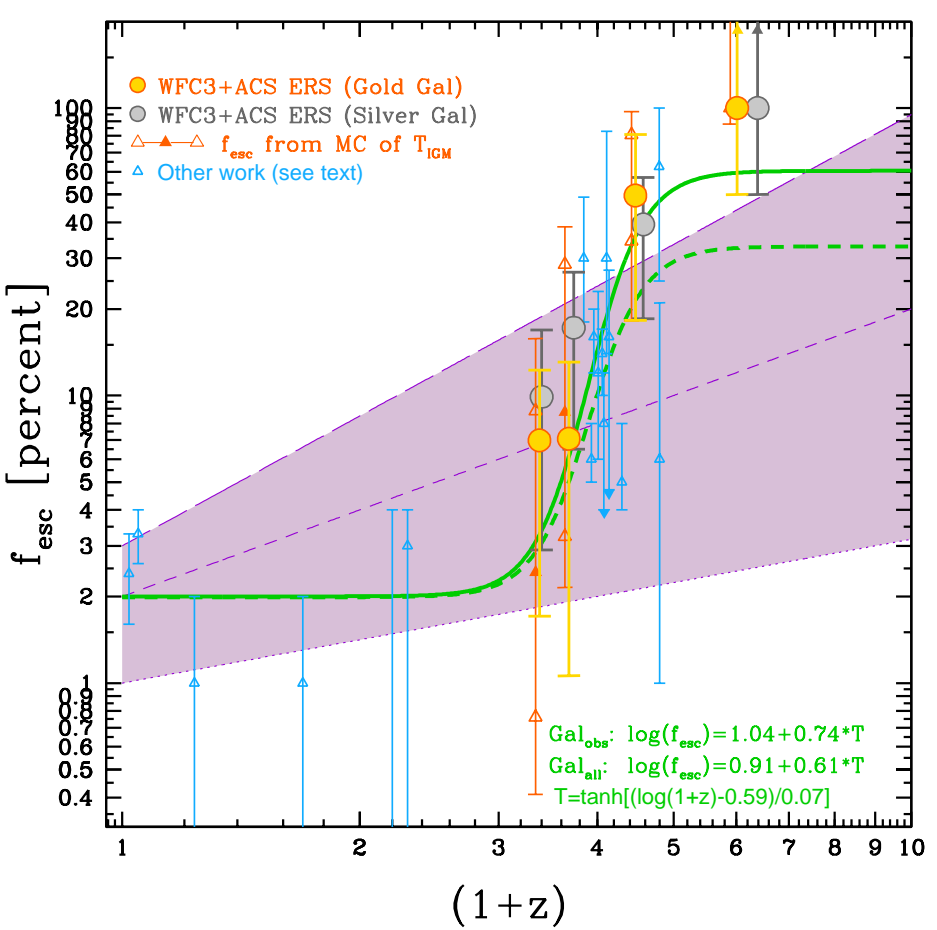
- Galaxies+AGN with $z_{\text{spec}} = 2.37 - 2.68$ represent $N(A_V)$ distribution.
- Spectroscopically selected galaxies + AGN at $z = 3.45 - 5.1$ miss $\sim 45\%$ of dusty ($A_V \gtrsim 1$ mag) objects at $z \gtrsim 3$.
- Our f_{esc} -value calculations vs. redshift will correct for this.

- (5) LyC Escape Fractions vs. z for Faint Galaxies & Weak AGN



PDFs of absolute & relative f_{esc} -values (Inoue⁺ 2014 MC), folding LyC fluxes $\pm 1\sigma$ errors through 10^9 random LOS of IGM transmission.

- Filled triangles indicate the resulting modal and circles the average f_{esc} -values in each PDF. Tick-marks show the $\pm 1\sigma$ -range.



[Left]: Relative f_{esc} -z: Published + ERS Gold & Gold+Silver samples.

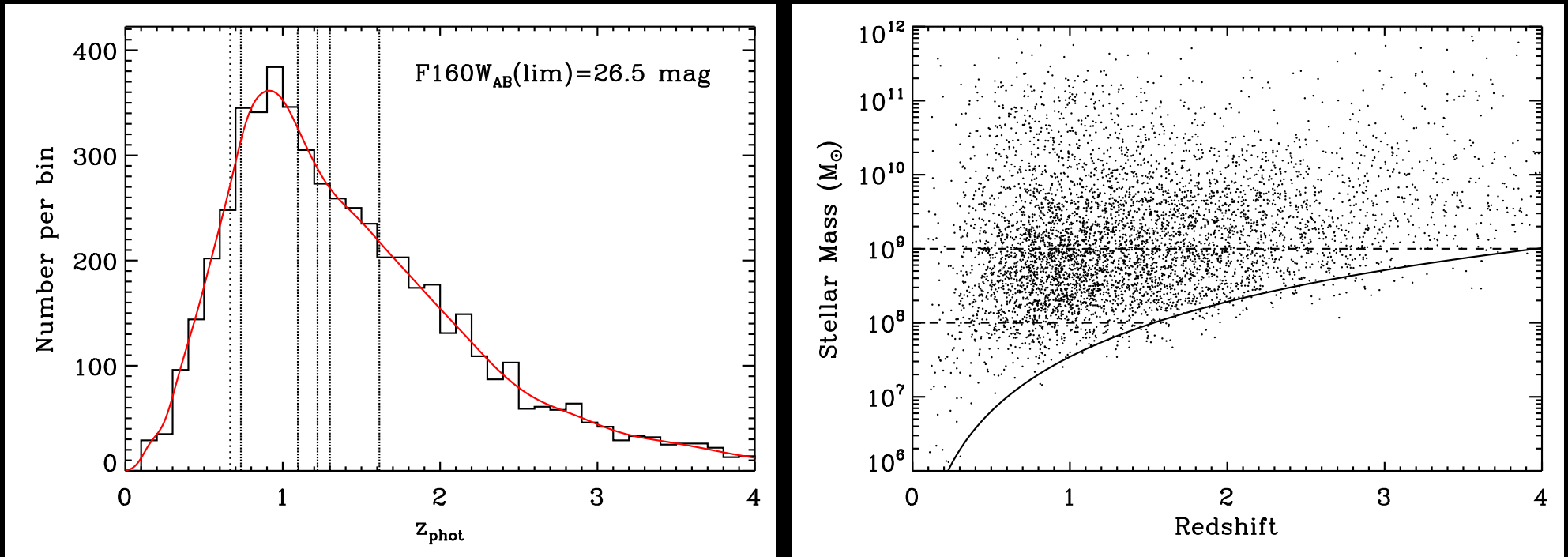
Shaded bounded by: $f_{\text{esc}} \simeq (0.02 \pm 0.01) \cdot (1+z)^{1.0 \pm 0.5}$ does not fit well.

Simple $\tanh[\log(1+z)]$ captures more sudden f_{esc} -increase at $z \gtrsim 2.5$ –3.

[Dashed: Same, corrected for $\sim 45\%$ missing SMGs($A_V > 1$) at $z \gtrsim 3.1$].

[Right]: Same for 12 AGN in ERS (+Bridge+ 2010) available thus far.

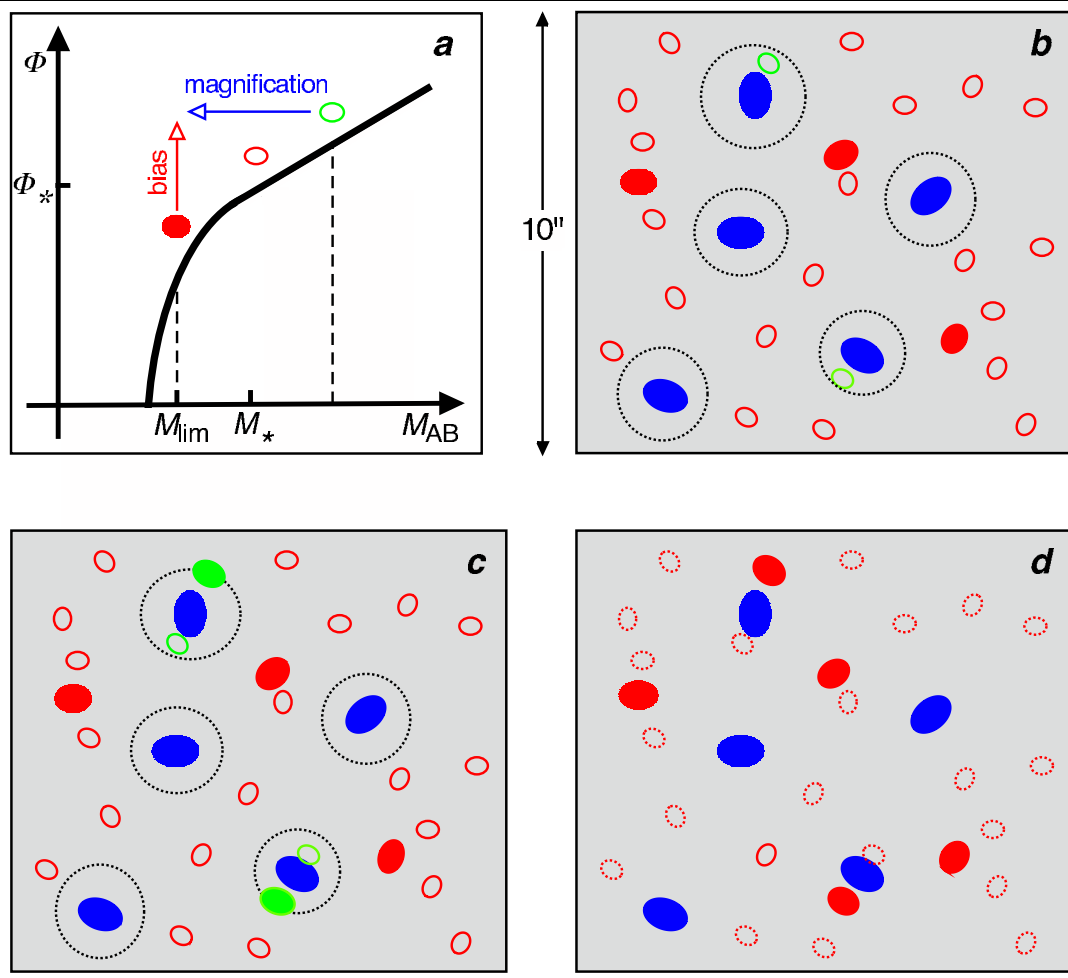
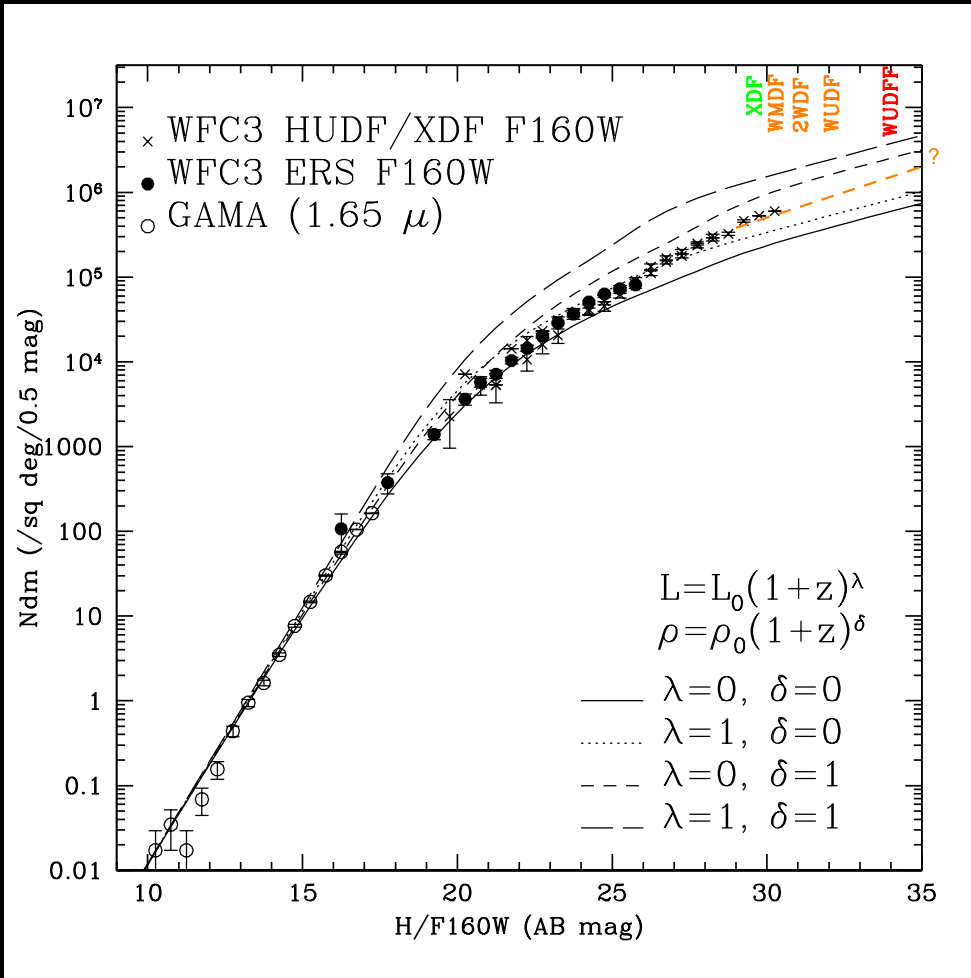
Object-weighted ratio of tanh-curves suggests f_{esc} (galaxies) high enough to dominate reionization at $z \gtrsim 3$, while AGN may dominate at $z \lesssim 2.5$.



WFC3 ERS 10-band redshift estimates accurate to $\lesssim 4\%$ with small systematic errors (Hathi et al. 2010, 2013), resulting in a reliable $N(z)$.

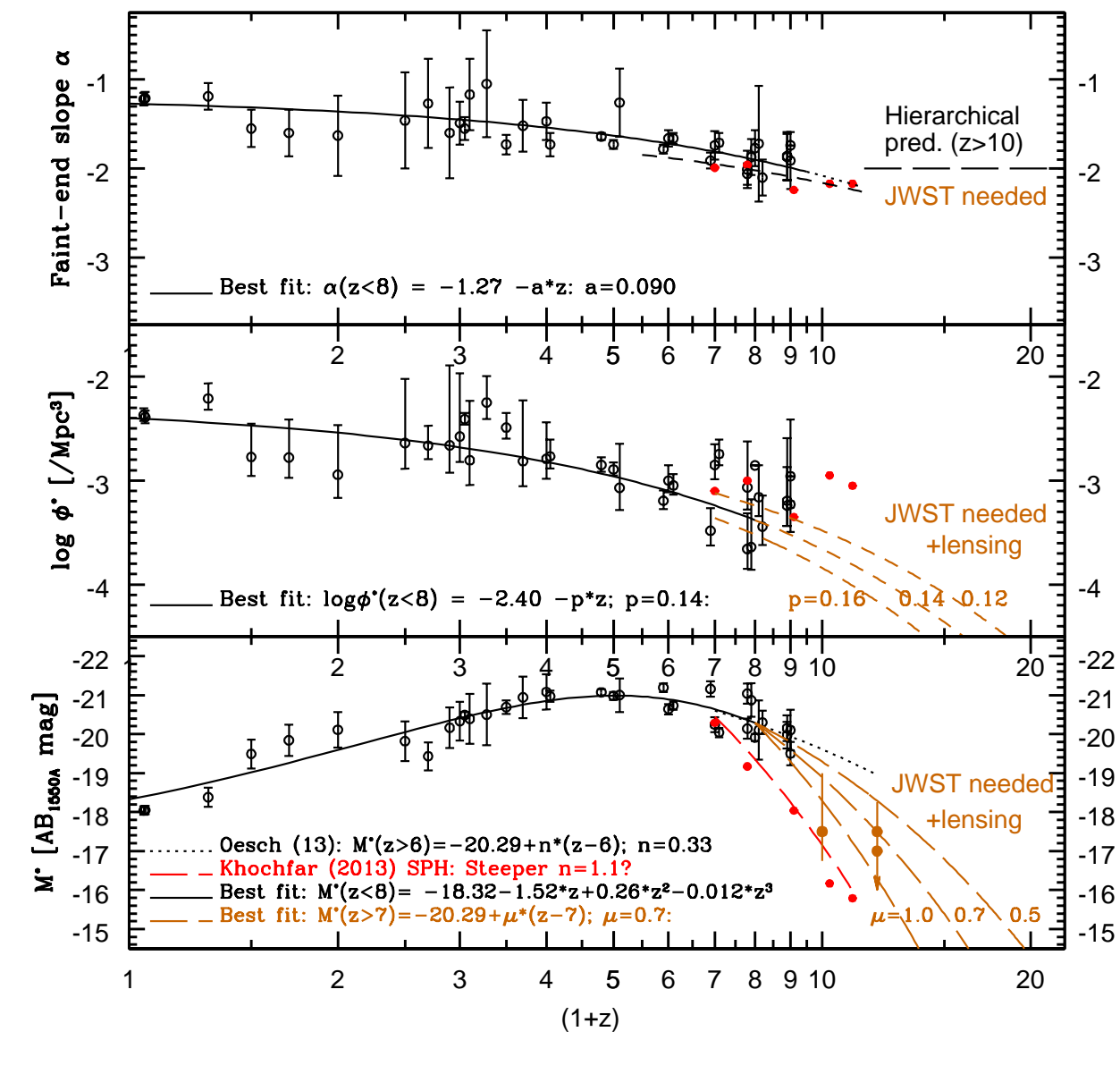
- Measure masses of faint galaxies to AB=26.5 mag, tracing the process of galaxy assembly: downsizing, merging, (& weak AGN growth?).
- ⇒ Median redshift in (medium-)deep fields is $z_{\text{med}} \simeq 1.5\text{--}2$.
- HUDF shows WFC3 $z \simeq 7\text{--}9$ capabilities (Bouwens⁺ 2014; Yan⁺ 2010).
- JWST will trace mass assembly and dust content $\lesssim 5$ mag deeper from $z \simeq 1\text{--}12$, with nanoJy sensitivity from 0.7–5μm.

(5b) Can JWST see most of the Reionizing sources?



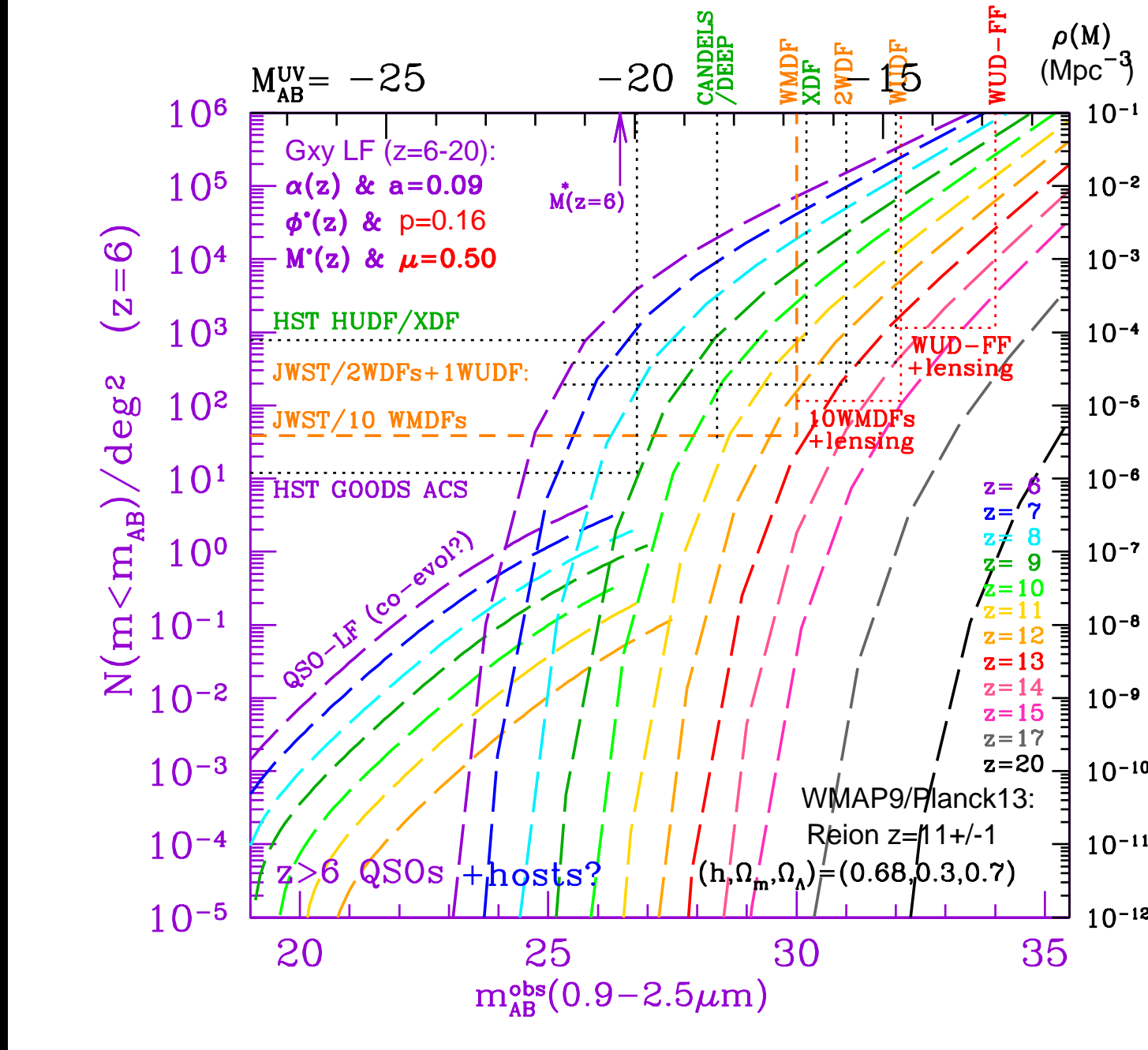
$1.6\mu\text{m}$ counts (Windhorst⁺2011). [F150W, F225W, F275W, F336W, F435W, F606W, F775W, F850LP, F105W, F125W, F140W not shown].

- Faint-end near-IR count-slope $\simeq 0.16 \pm 0.02$ dex/mag \longleftrightarrow Faint-end LF-slope $\alpha(z_{med} \sim 1.6) \simeq -1.4 \Rightarrow$ reach $M_{AB} \simeq -14$ mag.
- 800-hr WUDF can see $AB \lesssim 32$ objects: $M_{AB} \simeq -15$ (LMCs) at $z \simeq 11$!
- Lensing will change the landscape for JWST observing strategies (WUDFF).



Evolution of Schechter UV-LF: faint-end LF-slope $\alpha(z)$, $\Phi^*(z)$ & $M^*(z)$:

- For JWST $z \gtrsim 8$, expect $\alpha \lesssim -2.0$; $\Phi^* \lesssim 10^{-3}$ (Mpc^{-3}) (Bouwens⁺ 14).
 - HUDF: Characteristic M^* may drop below -18 or -17.5 mag at $z \gtrsim 10$.
- ⇒ Will have significant consequences for JWST survey strategy.



- Schechter LF ($6 \lesssim z \lesssim 20$) with best-fit $\alpha(z)$, $\Phi^*(z)$, $M^*(z)$ & $\mu=0.50$.
Area/Sensitivity for: HUDF/XDF, 10 WMDFs, 2 WDFs, & 1 WUDF.
- Will need lensing targets for WMDF–WUDFF to see $z \simeq 12\text{--}15$ objects.

(6) Summary and Conclusions

(1) HST can measure LyC for galaxies + weak AGN at $z \approx 2.26-5.5$.

- WFC3 and ACS filters designed with low-enough redleak to enable this.
- Samples of sufficient size ($N=11-118$) need to be stacked to see LyC signal.
- Astrometry/registration and sky-background subtraction must be carefully done in various stages.
- Subtle residual sky-gradients and other systematics ultimate limitation to LyC stacking (at $\gtrsim 32.3 \text{ mag arcsec}^{-2}$).
- Deepest 10-band images at HST resolution critical to mask-out all foreground interlopers to $AB \lesssim 27.5$ mag.
- Careful spectroscopic redshift selection critical for reliable samples.
- Must correct results for M_{AB} and A_V -biases that result from the necessary spectroscopic selection.

(2) LyC signal detected in sub-samples of $N=11\text{--}37$ objects at $z=2.26\text{--}5.5$.

- Detections of AB(LyC) generally better than $\gtrsim 3\text{--}4\sigma$ ($AB \simeq 29.5\text{--}31$ mag).
- Weak AGN have ~ 1 mag brighter AB(LyC), but are $4\text{--}10\times$ less numerous than galaxies.
- Stacked LyC SB-profiles are on average much flatter than the UV-continuum Sersic-profile.
- LyC may escape along few random sight-lines, offset from the average galaxy center.
- Non-Sersic LyC SB-profiles may indicate that the ISM porosity increases with r .

(3) Resulting f_{esc} -values show rapid “ $\tanh[\log(1+z)]$ ” increase at $z \gtrsim 2.5$.

- Dust-corrected SED-fits and MC simulations are essential to interpret this sudden drop in $f_{esc}(z)$.
- Best-fit 10-band ERS SEDs suggests A_V increases from $z \sim 6$ to $z \simeq 2.3$.
- Spectroscopic selection at $z=2.37\text{--}2.68$ follows field galaxy A_V , but at $z=3.45\text{--}5.1$ misses $\sim 45\%$ of dusty objects.
- This explains part, but not all, of the sudden f_{esc} -increase at $z \gtrsim 2.5$: Accumulating $A_V(t)$ may shut down $f_{esc}(z \lesssim 3)$.
- Object-weighted ratio of tanh-curves suggests f_{esc} (galaxies) high enough to dominate reionization at $z \gtrsim 3$, while AGN may take over at $z \lesssim 2.5$.

SPARE CHARTS

Table 2
LyC Stack Summaries of Gold and Combined Gold + Silver Samples

Filter (1)	<i>z</i> -range (2)	$\langle z \rangle$ (3)	N_{obj} (4)	LyC apertures				UVC apertures				
				m_{LyC} (5)	ABern (6)	SNR_{LyC} (7)	D_{LyC} (8)	m_{LyC} (9)	SNR_{LyC} (10)	D_{LyC} (11)	m_{UVC} (12)	SNR_{UVC} (13)
GOLD GALAXIES WITH AGN:												
F225W	2.291–2.291	2.291	1	30.12	0.46	2.34	0.213	30.00	1.10	1.424	27.90	7.85
F275W	2.470–3.008	2.697	7	28.92	0.12	8.77	1.372	29.56	6.97	0.665	25.00	156.9
F336W	3.217–3.474	3.349	3	29.69	0.30	3.58	0.690	29.53	4.74	0.492	24.45	118.2
F435W	4.760–4.823	4.792	2	28.58	0.24	4.48	0.571	>31.5	<2	0.357	24.66	79.0
GOLD GALAXIES WITHOUT AGN:												
F225W	2.302–2.450	2.380	14	29.98	0.19	5.64	1.059	30.00	4.80	1.451	24.43	237.5
F275W	2.559–3.076	2.682	11	30.09	0.19	5.71	0.656	29.80	4.90	1.583	24.51	192.2
F336W	3.132–3.917	3.472	11	30.66	0.24	4.48	0.259	30.21	3.75	0.895	24.88	101.9
F435W	4.414–5.786	5.015	15	30.37	0.33	3.28	0.354	30.61	2.32	0.467	26.12	70.3
ALL GOLD GALAXIES:												
F225W	2.291–2.450	2.374	15	29.92	0.17	6.53	0.958	30.01	4.93	1.407	24.50	240.8
F275W	2.470–3.076	2.688	18	29.61	0.10	10.40	0.782	29.31	10.32	1.427	24.68	226.2
F336W	3.132–3.917	3.446	14	30.13	0.24	4.56	0.943	29.82	6.01	0.923	24.75	131.0
F435W	4.414–5.786	4.989	17	29.51	0.22	4.87	0.874	30.70	2.25	0.468	25.79	95.3
GOLD + SILVER GALAXIES WITHOUT AGN:												
F225W	2.262–2.450	2.362	31	29.79	0.11	9.46	1.109	29.71	8.74	1.576	24.56	303.6
F275W	2.481–3.076	2.692	26	29.46	0.09	11.92	1.135	29.35	11.29	1.606	24.76	229.6
F336W	3.110–4.149	3.524	24	29.96	0.16	6.85	1.017	29.93	6.83	1.073	24.73	164.9
F435W	4.414–6.277	5.312	37	30.35	0.19	5.79	0.452	31.53	2.23	0.336	26.72	92.7
ALL GOLD + SILVER GALAXIES:												
F225W	2.262–2.450	2.362	33	29.88	0.12	9.27	1.017	29.72	8.63	1.620	24.59	295.7
F275W	2.470–3.076	2.669	33	29.34	0.07	15.11	1.082	29.22	14.03	1.627	24.79	252.7
F336W	3.110–4.149	3.505	27	30.01	0.16	6.94	1.036	29.93	7.19	1.089	24.68	188.2
F435W	4.379–6.277	5.263	40	29.84	0.15	7.33	0.669	30.08	5.83	0.668	26.22	103.1

Table 3
Summary of f_{esc} Constraints

$\langle z \rangle$	N_{obj}	$\langle f_{\text{LyC}}/f_{1500}(\text{Obs}) \rangle$	$\langle f_{1500}/f_{LyC}(\text{Int}) \rangle$	$A_V \text{med}$	$\langle T_{\text{IGM}} \rangle$	$f_{\text{esc},600}^{\text{rel}}$	$f_{\text{esc},700}^{\text{rel}}$	$f_{\text{esc}}^{\text{rel}}(\text{IGM-MC})$	$f_{\text{esc}}^{\text{abs}}(\text{IGM-MC})$
(1)	(2)	(3)	(4)	(5)	(6)	(7)	(8)	(9)	
GOLD GALAXIES with AGN:									
2.291	1	0.129 ± 0.0577	$3.44^{+0.13}_{-0.10}$	$0.90^{+0.14}_{-0.14}$	$0.297^{+0.081}_{-0.083}$	$\gtrsim 100\%$	$\gtrsim 100\%$	—	—
2.677	7	0.0270 ± 0.00309	$2.98^{+0.08}_{-0.07}$	$1.23^{+1.14}_{-1.13}$	$0.247^{+0.085}_{-0.085}$	$25^{+18\%}_{-16\%}$	$33^{+24\%}_{-22\%}$	—	—
3.349	3	0.00802 ± 0.00224	$11.4^{+0.20}_{-0.14}$	$0.10^{+0.14}_{-0.10}$	$0.112^{+0.049}_{-0.049}$	$79^{+48\%}_{-48\%}$	$82^{+50\%}_{-50\%}$	—	—
4.792	2	0.0158 ± 0.00389	$3.55^{+0.37}_{-0.26}$	$1.90^{+0.50}_{-0.50}$	$0.00108^{+0.00122}_{-0.00107}$	$\sim 100\%$	$\sim 100\%$	—	—
GOLD GALAXIES WITHOUT AGN:									
2.380	14	0.00213 ± 0.000568	$3.44^{+0.13}_{-0.10}$	$0.55^{+0.70}_{-0.44}$	$0.297^{+0.081}_{-0.083}$	$3.7^{+2.8\%}_{-2.8\%}$	$7.0^{+5.3\%}_{-5.3\%}$	$0.76^{+15}_{-0.35}$	$0.11^{+2.16}_{-0.05}$
2.682	11	0.00586 ± 0.00103	$2.98^{+0.08}_{-0.07}$	$0.58^{+0.89}_{-0.40}$	$0.247^{+0.085}_{-0.085}$	$5.3^{+4.5\%}_{-4.5\%}$	$7.1^{+6.0\%}_{-6.0\%}$	$3.22^{+35}_{-1.08}$	$0.27^{+2.96}_{-0.09}$
3.472	11	0.00488 ± 0.00109	$11.4^{+0.20}_{-0.14}$	$0.18^{+0.64}_{-0.12}$	$0.112^{+0.049}_{-0.049}$	$48^{+29\%}_{-29\%}$	$50^{+31\%}_{-31\%}$	34^{+63}_{-16}	32^{+57}_{-15}
5.015	15	0.0200 ± 0.00609	$3.55^{+0.37}_{-0.26}$	$0.17^{+0.67}_{-0.12}$	$0.00108^{+0.00122}_{-0.00107}$	$\sim 100\%$	$\sim 100\%$	$\sim 100\%$	$\gtrsim 21^{+79}_{-2}$
GOLD + SILVER GALAXIES WITHOUT AGN:									
2.362	31	0.00809 ± 0.000857	$3.74^{+0.12}_{-0.10}$	$0.55^{+0.70}_{-0.44}$	$0.306^{+0.055}_{-0.055}$	$5.2^{+3.7\%}_{-3.7\%}$	$9.9^{+7.0\%}_{-7.0\%}$	$1.76^{+15}_{-0.67}$	$0.26^{+2.22}_{-0.10}$
2.692	26	0.0132 ± 0.00111	$3.25^{+0.06}_{-0.06}$	$0.58^{+0.89}_{-0.40}$	$0.249^{+0.052}_{-0.054}$	$12.7^{+7.3\%}_{-8.2\%}$	$17^{+9.7\%}_{-10.7\%}$	$6.2^{+27}_{-2.1}$	$0.55^{+2.40}_{-0.18}$
3.524	24	0.00809 ± 0.00118	$4.33^{+0.34}_{-0.30}$	$0.18^{+0.64}_{-0.12}$	$0.089^{+0.027}_{-0.027}$	37^{+17}_{-20}	$39^{+18\%}_{-21\%}$	$6.5^{+25}_{-3.1}$	$24^{+68}_{-1.0}$
5.312	37	0.0353 ± 0.00611	$2.97^{+0.13}_{-0.15}$	$0.17^{+0.67}_{-0.12}$	$0.00019^{+0.00152}_{-0.00154}$	$\sim 100\%$	$\sim 100\%$	87^{+113}_{-55}	$\gtrsim 20^{+80}_{-2}$

- References and other sources of material shown:

<http://www.asu.edu/clas/hst/www/jwst/> [Talk, Movie, Java-tool]

<http://www.asu.edu/clas/hst/www/ahah/> [Hubble at Hyperspeed Java–tool]

<http://www.asu.edu/clas/hst/www/jwst/clickonHUDF/> [Clickable HUDF map]

<http://www.jwst.nasa.gov/> & <http://www.stsci.edu/jwst/>

<http://ircamera.as.arizona.edu/nircam/>

<http://ircamera.as.arizona.edu/MIRI/>

<http://www.stsci.edu/jwst/instruments/nirspec/>

<http://www.stsci.edu/jwst/instruments/fgs>

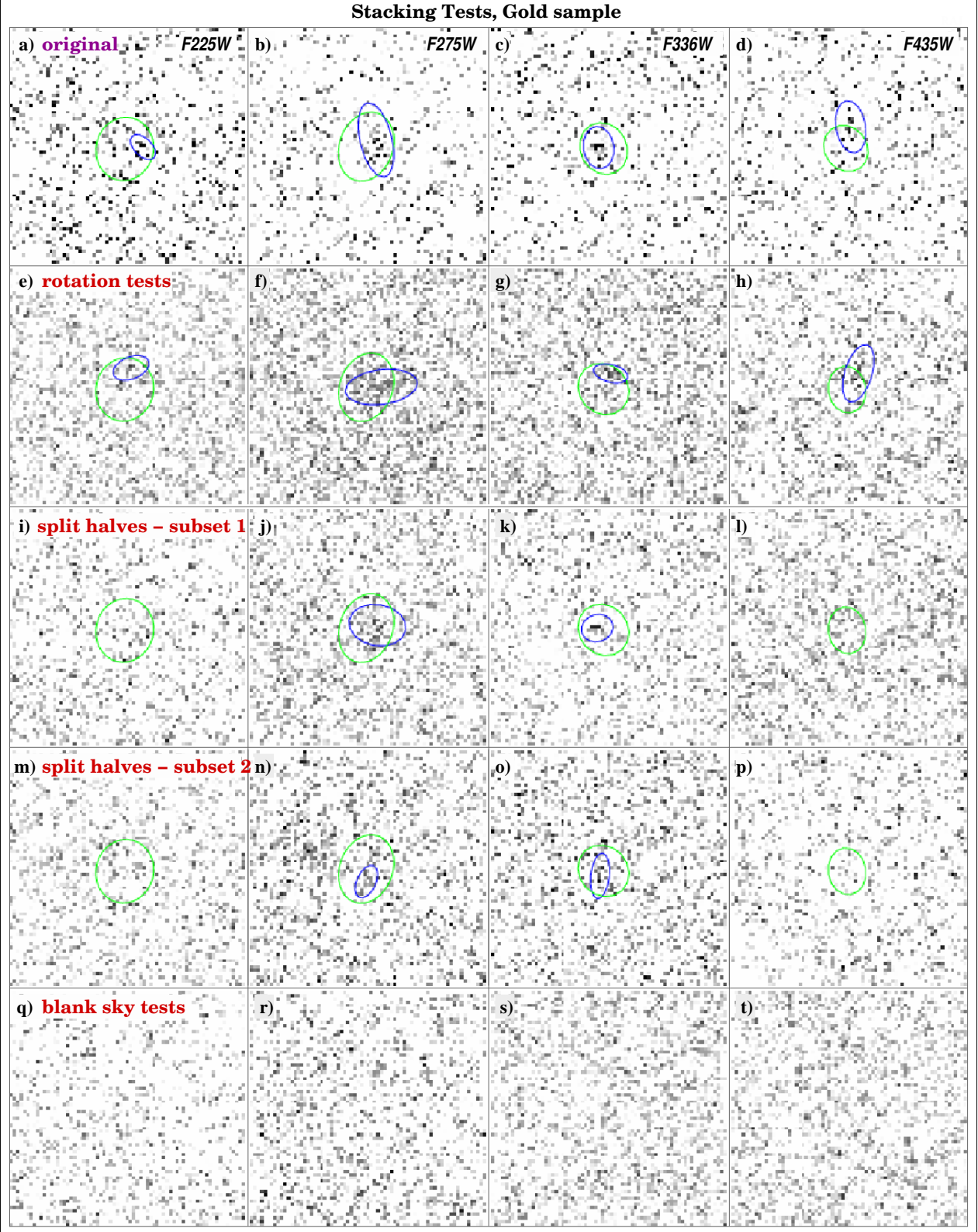
Gardner, J. P., et al. 2006, *Space Science Reviews*, 123, 485–606

Mather, J., & Stockman, H. 2000, *Proc. SPIE* Vol. 4013, 2

Windhorst, R., et al. 2008, *Advances in Space Research*, 41, 1965

Windhorst, R., et al., 2011, *ApJS*, 193, 27 ([astro-ph/1005.2776](#)).

Stacking Tests, Gold sample



$z=2.37$, $z=2.68$, $z=3.45$,
 $z=5.1$ Gold stacks;

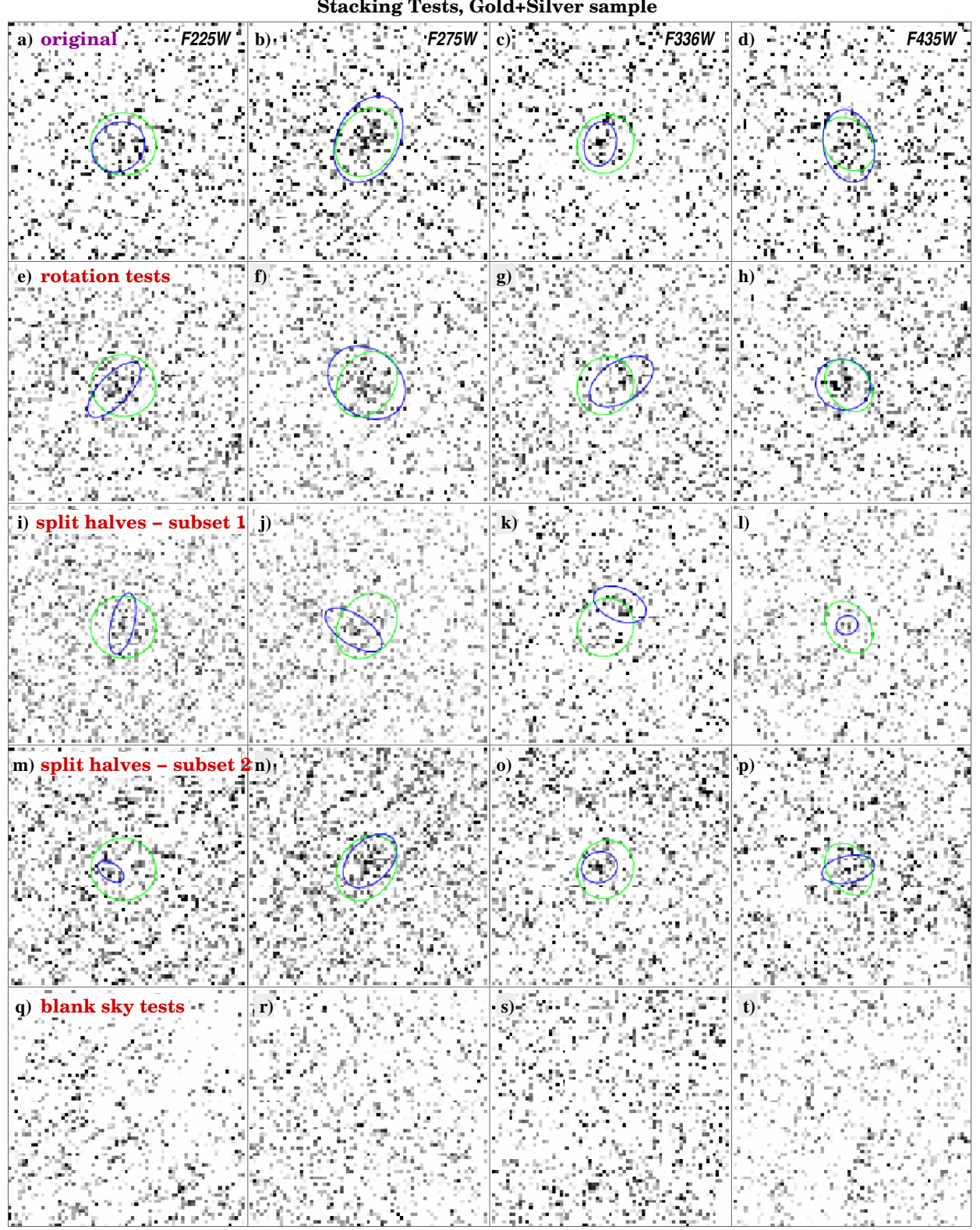
Same Gold stacks after random 90° rotation;

First independent data halves Gold stacks;

Second independent data halves Gold stacks;

Random sky-stacks to verify null-signal.

Stacking Tests, Gold+Silver sample



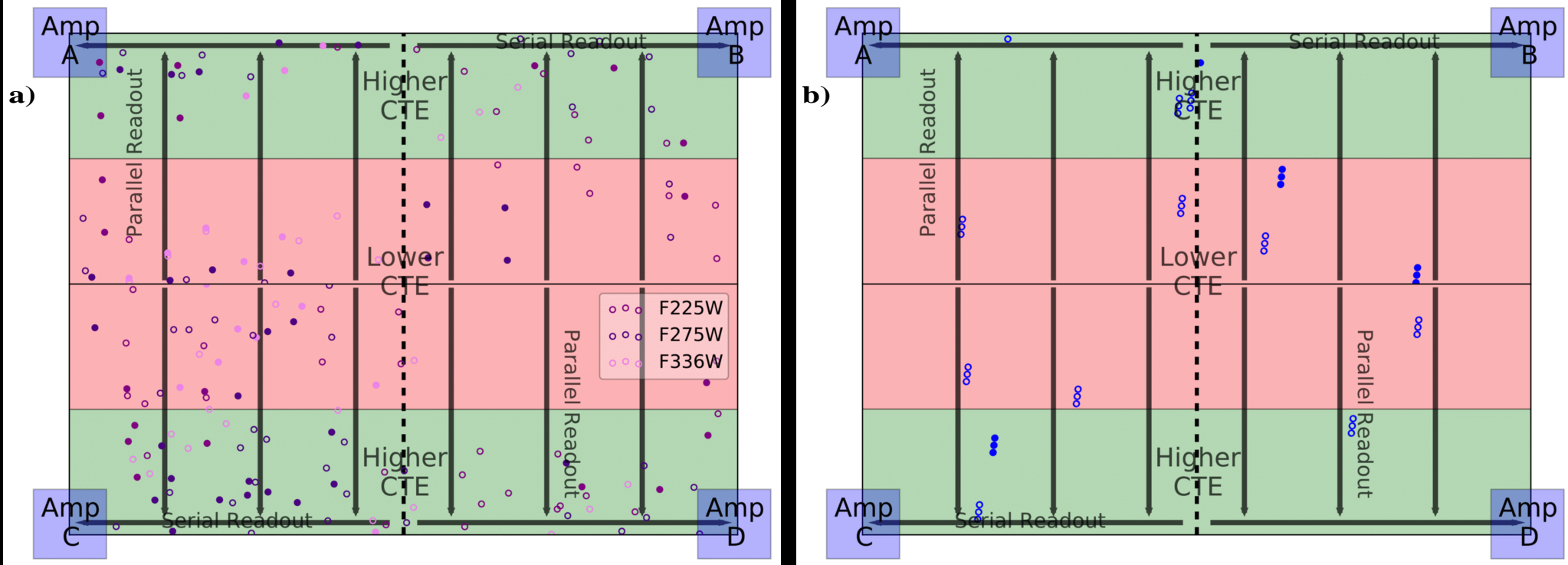
$z=2.37$, $z=2.68$, $z=3.45$,
 $z=5.1$ Silver stacks;

Same Silver stacks after
random 90° rotation;

First independent data
halves Silver stacks;

Second independent
data halves Silver stacks;

Random sky-stacks
to verify null-signal.



Detector location of “high-CTE” and “low-CTE” sub-samples: [LEFT]: WFC3/UVIS F225W, F275W, F336W. [RIGHT]: ACS/WFC F435W.

Green regions are closest to parallel read-out amplifier. Red regions are furthest from amplifiers, and may suffer more from CTE-degradation.

- Filled circles show marginal LyC signal in individual objects:
- These are fairly uniformly distributed across individual CCDs.

Average stacked LyC diff: $\Delta(\text{Lower-CTE} - \text{High-CTE}) \simeq 0.5 \pm 0.35$ mag.

⇒ Less than four months after WFC3’s launch, CTE-induced systematics are not yet larger than the random errors in the LyC signal.